

A Practical Approach to Assess the Wildfire Ignition and Spreading Capacities of Vegetated Areas at Landscape-scale

Artan Hysa (✉ ahysa@epoka.edu.al)

Epoka University

Velibor Spalevic

University of Montenegro

Branislav Dudic

Comenius University

Sanda Roşca

Babeş-Bolyai University

Alban Kuriqi

University of Lisbon

Ştefan Bilaşco

Babeş-Bolyai University

Paul Sestras

Technical University of Cluj-Napoca

Research Article

Keywords: climate change, disaster risk reduction, fuel, QGIS, remote sensing

Posted Date: March 1st, 2021

DOI: <https://doi.org/10.21203/rs.3.rs-264516/v1>

License: © ⓘ This work is licensed under a Creative Commons Attribution 4.0 International License.

[Read Full License](#)

A Practical Approach to Assess the Wildfire Ignition and Spreading Capacities of Vegetated Areas at Landscape-scale

Artan Hysa^{1,*}, Velibor Spalevic², Branislav Dudic^{3,4*}, Sanda Roșca⁵, Alban Kuriqi^{6*}, Ștefan Bilașco^{5,7}, Paul Sestras⁸

^{1*} Faculty of Architecture and Engineering, Epoka University, Tirana, Albania; ahysa@epoka.edu.al

² Geography Department, Faculty of Philosophy, University of Montenegro, 81400 Niksic, Montenegro; velibor.spalevic@ucg.ac.me

³ Faculty of Management, Comenius University in Bratislava, 82005 Bratislava, Slovakia

⁴ Faculty of Economics and Engineering Management, University Business Academy, 21102 Novi Sad, Serbia; branislav.dudic@fm.uniba.sk

⁵ Faculty of Geography, Babes-Bolyai University, 400006 Cluj-Napoca, Romania; sanda.rosca@ubbcluj.ro (S.R.), stefan.bilasco@ubbcluj.ro (Ș.B.)

⁶ CERIS, Instituto Superior Técnico, Universidade de Lisboa, 1049-001 Lisbon, Portugal; albankuriqi@gmail.com

⁷ Cluj-Napoca Subsidiary Geography Section, Romanian Academy, 400015 Cluj-Napoca, Romania, stefan.bilasco@ubbcluj.ro

⁸ Faculty of Civil Engineering, Technical University of Cluj-Napoca, 400020 Cluj-Napoca, Romania; psestras@mail.utcluj.ro

Abstract

We bring a practical and comprehensive GIS-based framework to utilize freely available remote sensed datasets to assess wildfire ignition probability and spreading capacities of vegetated landscapes. The study area consists of the country-level scale of the Romanian territory, characterized by a diversity of vegetated landscapes threatened by the consequences of climate change. We utilize the Wildfire Ignition Probability/Wildfire Spreading Capacity Index (WIPI/ WSCI). WIPI/ WSCI models rely on a multi-criteria data mining procedure assessing the social, environmental, geophysical, and fuel properties of the study area based on open access remote sensed data. We utilized the Receiver Operating Characteristic (ROC) analysis to weigh each indexing criterion's impact factor and assess the model's overall sensitivity. Introducing ROC analysis at an earlier stage of the workflow elevated the final Area Under the Curve (AUC) of WIPI from 0.705 to 0.778 and WSCI from 0.586 to 0.802. The modeling results enable discussion on the vulnerability of protected areas and the exposure of man-made structures to wildfire risk. Our study shows that within the wildland-urban interface of Bucharest's metropolitan area, there is a remarkable building stock like healthcare, residential and educational that are significantly exposed to wildfire spreading the risk.

Keywords: climate change; disaster risk reduction; fuel; QGIS; remote sensing.

31 1. Introduction

32 Climate change and global warming are expected to affect natural hazards like flooding and wildfires
33 worldwide. These may have multiplied domino effect consequences on other natural and urban systems
34 leading to severe disasters at local scales ¹⁻³. While the emergence of flooding events relies mostly on the
35 weather conditions and the natural/ artificial properties of the catchment area, wildfires implicate human
36 behavioral activities. The multifaceted character of the wildfire phenomena is acknowledged in the literature.
37 Chapin et al. ⁴ define wildfire as a wicked problem. According to Levin et al. ⁵, wildfires are multi-layered
38 phenomena that implicate diverse interacting cycles between causes and effects acting in certain territories.
39 Identifying the relevant factors that significantly correlate with the wildfire regimes remains a critical
40 challenge to scientists ⁶⁻⁸.

41 In the classical wildfire assessment approach, the interaction of favorable weather conditions with the
42 study area's geophysical and fuel properties is considered the core prerequisite of the fire environment triangle
43 ⁹. Lightning strikes are the primary igniters ¹⁰. However, most wildfires are reported to have been caused by
44 human activity, either intentionally or accidentally ¹¹. Human activity patterns have become a determinant
45 during the wildfire ignition phase ^{12,13}.

46 Mansuy et al. ¹⁴ contrast the anthropogenic factors to the macro-environmental ones and report that the
47 human footprint affects almost equal wildfire risk both inside and outside the North-American protected
48 landscapes. The consequences of human activities on fire regimes are reported to leave under shadow the
49 effects of climate change ¹⁵. The effect of societal habits like the Daylight-Saving Time (DST) alterations have
50 been acknowledged to upsurge the number of wildfire ignitions. For example, Kountouris ¹⁶ reports that DST
51 transition during the Spring season has increased the number of non-prescribed wildfire ignitions by about
52 30% in the US, relying on around 2 million wildfire ignition of 23 years records.

53 A more recent study presents the impact of COVID-19 lockdown on the wildfire regimes in a wildfire-
54 prone region like the Mediterranean ^{3,17}. The authors report a significant decrease in the total burned area
55 during this period compared to the estimations that counted for similar drought-related circumstances to
56 previous years. The decrease in social activities has resulted in a significant reduction of wildfire events. Thus,

57 the integration of anthropogenic factors within the wildfire risk assessment tools has become indispensable to
58 increase the models' sensitivity ¹⁸.

59 Although the anthropogenic factors that impact wildfire events have gained considerable attention in the
60 literature, their combined usage alongside hydro-meteorological and biophysical factors in wildfire spreading
61 capacities models is not spread enough. In this study, we shortlisted sixteen criteria about the anthropogenic
62 (S-social), hydro-meteorological (E-environmental), geophysical (P-physical), and fuel (F) properties of the
63 study area (Romania) following our earlier GIS-based method ¹⁹. Through literature review and evaluating the
64 available open access geospatial data, we considered the following criteria; population density (S1), distance
65 to settlements (S2), distance to transportation network (S3), distance to main roads (S4), agriculture distance
66 (S5), solar radiation (E1), precipitation (E2), maximum temperature (E3), wind speed (E4), slope (P1), aspect
67 (P2), altitude (P3), distance to water sources (P4), fuel type (F1), tree cover density (TCD) (F2), and
68 normalized difference vegetation index (NDVI) (F3), Unlike our previous studies ^{19,20}, we introduced
69 population density as a new criterion within the wildfire ignition probability/ wildfire spreading capacity index
70 (WIPI/WSCI) model, considering that the current literature tightly correlates the population density and the
71 wildfire ignition risk ^{21,22}.

72 This study aims to develop a comprehensive and practical GIS-based model for assessing the wildfire
73 ignition and spreading capacities based on freely available geospatial data. The proposed model is aimed to
74 be reproducible to other vegetated surfaces where the remotely sensed data are available. Another goal is to
75 test the utility of the ROC/AUC method in weighting each criterion's impact factor by comparing it with the
76 analytic hierarchy process (AHP) that has been widely used in previous studies. Here we aim to deliver
77 tangible graphical (maps) and statistical results about the wildfire ignition and spreading capacities in
78 Romania, supporting disaster risk reduction agendas nationwide.

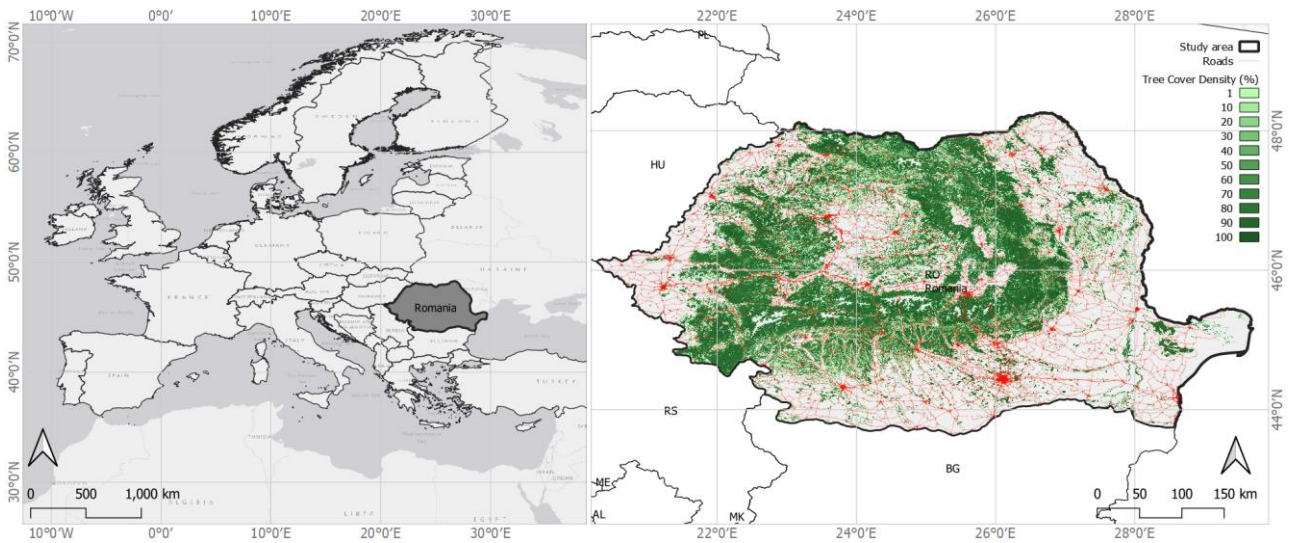
79 **2. Materials and Methods**

80 *2.1. Study Area*

81 The study area is represented by Romania's territory, a country located in the central-eastern part of
82 Europe with an area of 238391 km² (Fig. 1). Romania has a vast diversity of landforms, each with

83 representative forestry variation, which includes: the Transylvanian Depression located in the center of the
84 Carpathian Mountains arc, a territory that offers the right conditions for the development of deciduous forests,
85 i.e., with species such as *Carpinus betulus*, *Fagus sylvatica*, *Tillia tomentosa*, *Ulmus minor*, *Quercus petraea*
86 extended over large areas). The Romanian Carpathian Mountains (RCM) occupy 57% of the country's
87 territory, where extensive forests are spread over large areas.

88 According to Romanian legislation, a forest is considered an area of at least 0.25 hectares of land occupied
89 by forest vegetation. The mature specimens reach 5m in height under normal vegetation conditions and have
90 a coverage index (consistency) of more than 10% (0.1). To these territories are added the areas covered with
91 junipers (*Juniperus*) in the high mountain area of over 1800-2000m in altitude and forest protection curtains
92 with more than 0.5 hectares and a width of more than 20 meters. Forest protection curtains are accepted crucial
93 interventions in forest protection policy. They are projected to have a significant protective effect on Romanian
94 forest cover on the brink of climate change ²³.



95
96 **Figure 1.** Romania within Europe (a), and Romanian territory including tree cover density (TCD) and
97 transportation network distribution (b).

98 At the territorial level of Romania, 29.9% of the surface is covered by different forests, covering 7.13
99 million hectares ²⁴. Romania is one of the countries with the highest percentage of occupied forest areas, with
100 the latest estimates having a significant growth rate (19.3 million m³/year for conifers, 19 million m³/year for
101 beech, 8.1 m³/year for quercinea, 8.6 million m³/year for hardwoods and 3.4 million m³/year for softwoods),
102 to which are added old forests and virgin forests in different stages of conservation. Large forest areas are

103 predominantly in the mountainous and hilly areas and areas with lower altitudes. There is a higher density of
104 human settlements, a crucial aspect considering the present study's objectives. We have included further details
105 about Romania's forest structure in Table S1 (see Supplementary files online).

106 Changes over time in the areas covered by forest are under the direct influence of natural factors such as
107 the influence of climate change on the consistency and composition of forests, the migration of forest species
108 beyond known ecological limits, the negative influence of floods with short return periods, the decrease of
109 physical and chemical properties of soils due to soil erosion and vegetation fires with natural causes. Anthropogenic
110 changes are also present due to deforestation caused by logging, legal and illegal, whose rate increased after
111 2000^{25,26}. However, some territories showed a forest gain due to the afforestation of large areas of abandoned
112 pastures²⁶. Furthermore, the Spatio-temporal evolution of forest cover in Romania is tightly correlated with
113 the forest management regimes affected by socio-political fluctuations starting from the early 19th century²⁷.

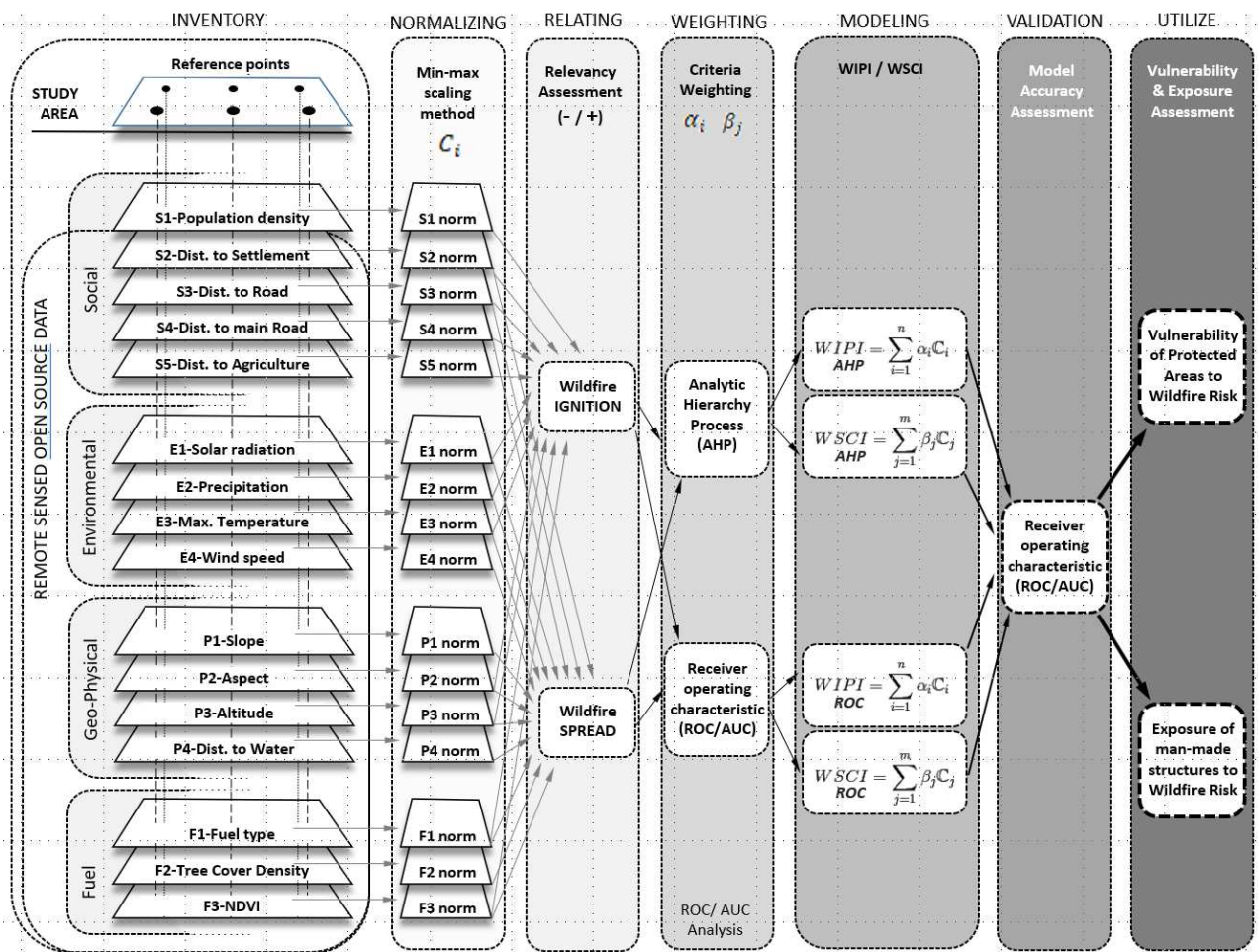
114 2.2. WIPI/ WSCI model and the current updates

115 This study methodologically relies on the Wildfire Ignition Probability/ Wildfire Spreading Capacity
116 Index (WIPI/ WSCI). Initially, the method defines criteria that have proven relation with either the wildfire
117 occurrence or behavior. The number of criteria varies according to the available data and the specifics of the
118 study area. Each reference point location within the vegetated surface is loaded with unique absolute values
119 through a multi-criteria inventory procedure¹⁹. Each criterion's relative weighted factor was initially assigned
120 via Analytical Hierarchy Process (AHP) pairwise comparison method. The sensitivity of the model has been
121 assessed via ROC/AUC method in another study focusing on the case of Montenegro²⁸.

122 Fig. 2 presents the methodical workflow of this study. It includes the updates that we push forward as
123 improvements of WIPI/ WSCI, applied in Romania's case. At this stage, the workflow consists of seven
124 sequential stages. Besides the inventory procedure, the first stage includes defining the vegetated surfaces
125 within the study area and the reference points that spatially represent the vegetation surfaces. The reference
126 points serve as data collecting pivots loaded with all 16 criteria' unique values, as shown in Fig. 2. The unequal
127 range of inventory values necessitates a normalizing procedure before indexing calculations. This stage
128 equalizes the range of inventory values of each criterion into a gradient between 0 and 1. The max/min

129 normalizing procedure is selected as it is accepted as the most right and straightforward method for well-
 130 known sets of records ²⁹.

131 The third stage consists of subgrouping the criteria into two sets according to their relationship with either
 132 wildfire ignition or spreading (see Fig.2, third stage). This division is based on a literature review shown in
 133 our earlier work ¹⁹. Moreover, a relevancy indicator is given to each criterion according to their direct or
 134 indirect relationship with wildfire regimes. This is explained in detail in Table 1. The first three methodical
 135 stages are borrowed from our previous studies.



136
 137 **Figure 2.** Workflow seven stages of the method.
 138

139 In the fourth stage, we propose ROC/AUC analysis (via SPSS software) as a weighting method among
 140 criteria, besides the analytic hierarchy processing (AHP) pairwise comparison method. This relies on the

141 specific characteristics of the study area and historical data on fire regimes. Indexing values are calculated as
142 the sum of the products between inventory value and each criterion's impact factor, as shown in Eq.1 and 2.

143

$$WIPI = \sum_{i=1}^n \alpha_i C_i \quad (1)$$

144 Where; WIPI is the normalized wildfire ignition probability index, C_i is the inventory value of criterion i ,
145 α_i the weighted impact coefficient of criterion i .

146

$$WSCI = \sum_{j=1}^m \beta_j C_j \quad (2)$$

147 Where; WSCI is the normalized wildfire spreading capacity index, C_j is the inventory value of criterion
148 j , β_j weighted impact coefficient of criterion j .

149 We compare the earlier model results (WIPI/ WSCI) and the updated one (WIPI_ROC / WSCI_ROC) as
150 applied in Romania's case. During the sixth stage, the ROC/AUC method is used to assess both models'
151 accuracy, leading to a comparative discussion. At the final stage, the WSCI_ROC model results are used in
152 vulnerability assessment of protected areas and exposure analysis of urbanized zones.

153 2.3. Data acquisition

154 This study depends on a variety of free access to remotely sensed geospatial data. These data are acquired
155 from various sources. We have included detailed information in Table S2 (Supplementary files online), which
156 presents the full list of the data name, data type, Minimum Mapping Unit (MMU), the source, and utility
157 within the method's workflow. CORINE Land Cover (CLC) is a pan European vector data provided by the
158 European Environment Agency (EEA), which delivers a hierarchical classification of 44 land cover types ³⁰.
159 The classification method simultaneously utilizes the Sentinel-2 satellite imagery (i.e., the 1st dedicated
160 European satellite for land monitoring) Landsat-8 images for gap-filling. In this study, we rely on the data of
161 2018 to gather geospatial information about vegetation surfaces, settlements (S2), fuel type (F1), and
162 agricultural areas (S5). EEA supplies other data such as Digital Elevation Model (DEM) and Tree Cover
163 Density (TCD). DEM is delivering information about slope (P1), aspect (P2), and altitude (P3) in raster format
164 of 25m in resolution.

165 Normalized Difference Vegetation Index (NDVI) data is extracted from the Terra Moderate Resolution
166 Imaging Spectroradiometer (MODIS) Vegetation Indices (MOD13Q1) Version 6. These data are produced in
167 a resolution of 250m by choosing the most reliable pixel value among daily values within 16 days. The low
168 percentage of cloud coverage, low view angle, and the highest NDVI value are among the applied selection
169 criteria^{31,32}. In this study, we used the period between 28 July and 12 August within the fire season of 2018.

170 Raster data about solar radiation (E1), precipitation (E2), maximum temperature (E3), and wind speed
171 (E4) are derived from Worldclim 2.0 database (<http://www.worldclim.com/version2>). It consists of raster
172 images of 30s resolution that provide monthly average values recorded between 1970 and 2000³³. In this study,
173 we use August's average records as the weather conditions for wildfire spread are highest. The remaining
174 criteria, like distance to water (P4) and transportation network (S2 & S3), stand on Open Street map (OSM)
175 data enabled for free via the Geofabrik portal.

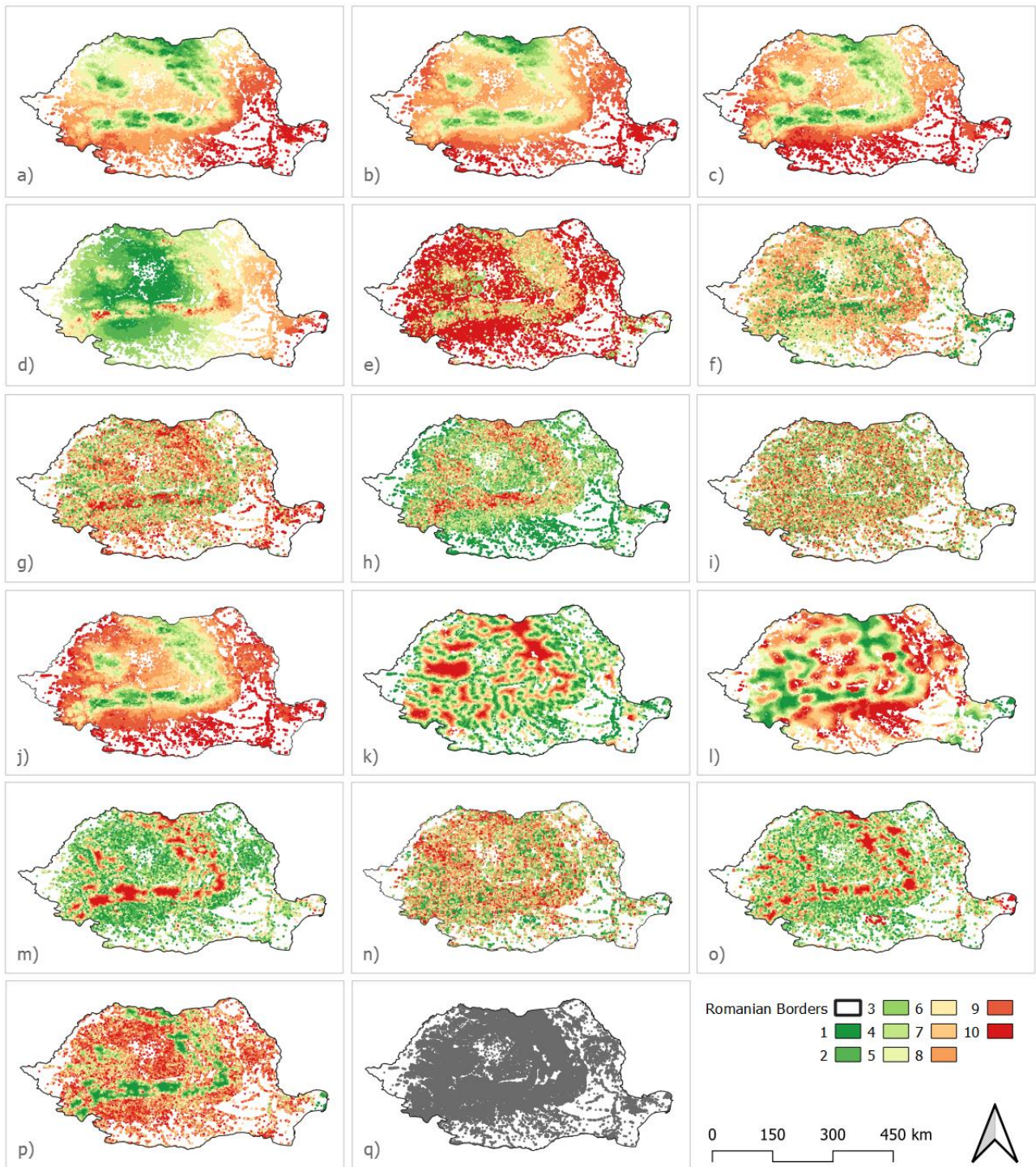
176 The population density information is produced based on population records at the smallest local
177 administrative unit level, as shown in Fig. S1 (Supplementary files online) based on the data provided by the
178 National Institute of Statistics of Romania. Another crucial piece of data used in this study is the Burned Area
179 (BA) products acquired from Copernicus Climate Change Service (2019). They provide information about the
180 total BA at the pixel level (250 m). The results are prepared via reflectance change analysis of medium
181 resolution sensors like Terra MODIS, Sentinel-3 OLCI combined with the thermal data by MODIS. These
182 products are vital raw data for research that focuses on themes like climate change, land use and land cover
183 dynamics, wildfire risk assessment, among others³⁴. MODIS products are the most widely used global dataset
184 by the scientific community³⁵⁻³⁷. According to Fig. S2, 70410 reference points overlap with the vegetated
185 surfaces. Further details about the data curating are included in the supplementary files online.

186 **3. Results**

187 *3.1. Multi-criteria Inventory of wildfire-related factors in Romania*

188 First, the method delivers inventory results on an individual level per each criterion. Fig. 3 presents the
189 relative wildfire proneness map of vegetated surfaces (Fig. 3q) in Romania based on each criterion. The color
190 palette is set as the gradient of red-yellow-green, where red shows the highest risk areas while green the least

191 risk. The gradient is assigned according to the relative indicator, as explained in Table 1. For example, criteria
 192 like solar radiation (E1) and precipitation (E2) are shown under reversed color gradient. In other words, the
 193 highest solar radiation values indicate the highest risk. In contrast, the highest precipitation records correlate
 194 with the lowest risk.
 195



196

197 **Figure 3.** The relative risk of vegetated surfaces (q) in Romania for each criterion; (a) solar radiation, (b) precipitation,
198 (c) maximum temperature, (d) wind speed, (e) fuel type, (f) tree cover density, (g) NDVI, (h) slope, (i) aspect, (j) altitude,
199 (k) distance to water, (l) distance to urban centers, (m) distance to settlements, (n) distance to any road, (o) distance to
200 main roads, (p) distance to agriculture.
201

202 According to Fig.3, the RCM that cross the Romanian territory in the central region from north to south-
203 west direction stand as a determinant of the spatial distribution of the relative risk for the majority of the
204 criteria. First, the hydro-meteorological criteria visually correlate with the topography of the study area. Fig.
205 3a shows that solar radiation (E1) is higher at lower altitudes, especially in the south-east of RCM, and lower
206 at high altitudes. Similarly, the recorded maximum temperatures (E3) are on the same line with the altitude
207 (P3) values presented in Fig. 3j.

208 Wind speed (E4) is the only environmental criterion that is not tightly correlated with altitude (Fig. 3d).
209 The slopes of RCM face south and south-east and remain an exposed area to winds flowing from the Black
210 Sea and the Mediterranean. Similarly, the remaining plain territories in Romania's south-eastern region facing
211 the Black sea are exposed to considerable average wind speeds compared to the north-western plains (Fig.
212 3d). Among geophysical criteria, slope (P1) is the only criterion that correlates with the altitude values (Fig.
213 3h). Most of the sloped surfaces are found along with the RCM layout. Whereas the aspect (P2) values are
214 more uniformly dispersed in the territory (Fig. 3i) and distance to water surfaces (P4) follows the spatial
215 distribution of water elements in the landscape (Fig. 3k), independently to the altitude values.

216 3.2. *Calibrated weighting of Criteria*

217 For the previous version, we adopted the weighted factors as assigned via an AHP pairwise comparison
218 method ²⁸, as listed in Table 1. Besides, the revised weighted impact factors are assigned according to each
219 criterion's sensitivity analysis concerning the historical fire regimes. Fig. 4 presents the ROC analysis values
220 per each criterion under four groups; hydro meteorological- environmental (E), fuel (F), geophysical (P), and
221 anthropogenic- social (S).

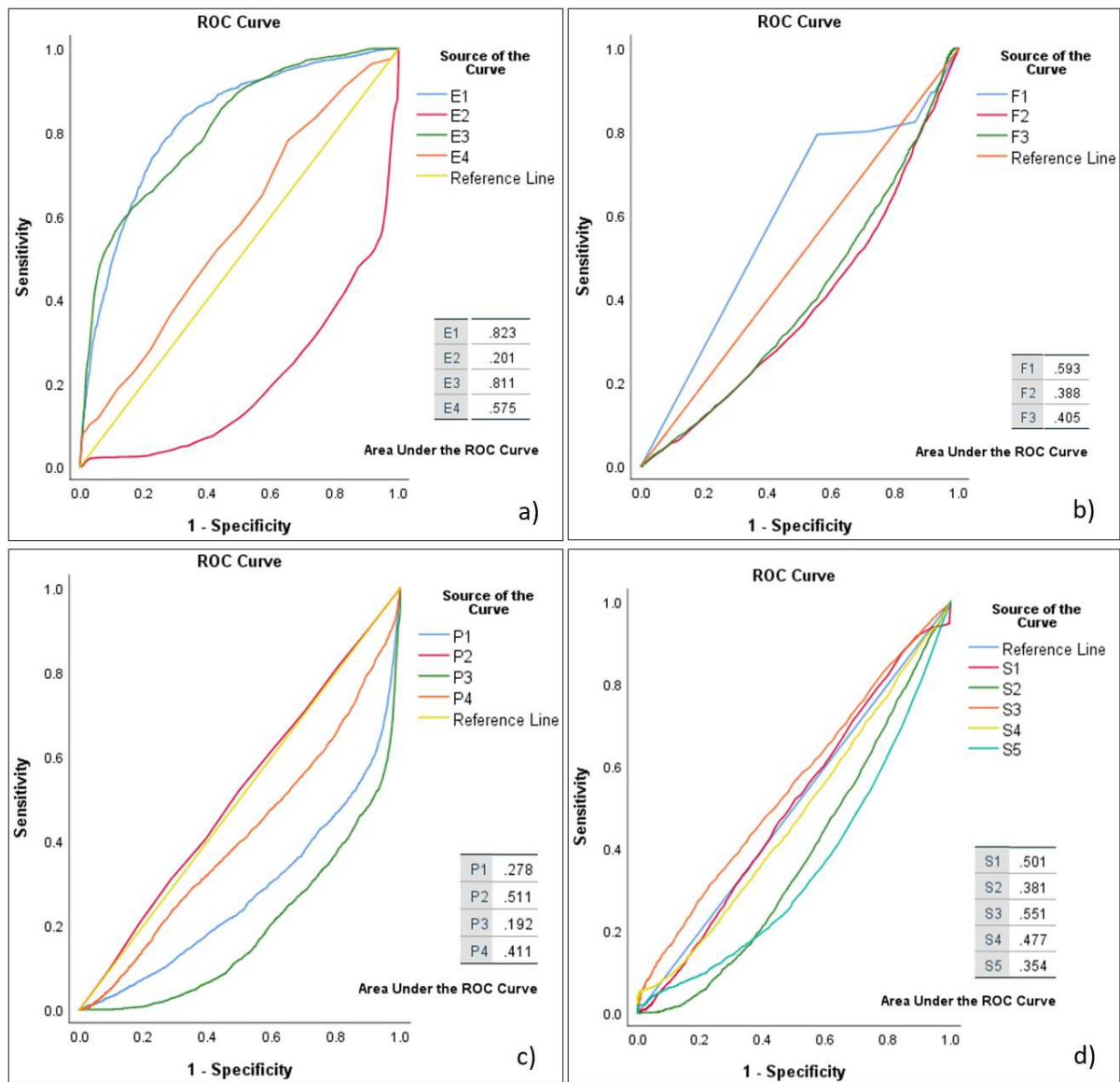


Figure 4. ROC curve analyses for (a) hydro-meteorological (E1-solar radiation, E2-precipitation, E3-maximum temperature, E4-wind speed), (b) fuel (F1-fuel type, F2-tree cover density, F3-ndvi), (c) geophysical (P1-slope, P2-aspect, P3-altitude, P4-distance to water), and (d) anthropogenic/ social (S1-population density, S2-distance to settlements, S3-distance to any road, S4-distance to main roads) factors about burned regime values.

222

223

224

225

226

227

228

229

230

231

232

233

234

The sensitivity analysis is performed in SPSS software via the ROC analysis tool. According to the inventory phase results, there are 70410 reference point locations within Romania's vegetated surfaces. The distance between points is 1km, and each point represents a vegetated surface of 1km². One thousand nine hundred fifty-six points have a five-year cumulative burned area fraction (2015-2019) value above 100%. These points are considered positive samples in the ROC analysis procedure in finding each criterion's sensitivity.

235 The results presented in Fig. 4 reveal the hypothetical models' sensitivity that has a single determinant,
 236 being each criterion. It is a way to find the correlation between inventory measurements of each criterion with
 237 the burned area fraction in Romania (see Fig. S2 in Supplementary files online). According to Fig.4, the
 238 highest AUC value belongs to E1 (solar radiation) and E3 (maximum temperature), respectively 0.823 and
 239 0.811. In other words, it means that a model that was based just on the criterion of solar radiation would have
 240 a predictability of 82%. While, the lowest AUC values are recorded for E2 (precipitation), P1 (slope), and P3
 241 (altitude), respectively, 0.201, 0.278, and 0.192. In principle, the lowest the AUC value, the lowest the
 242 correlation between the criterion and the wildfire recorded burned area fraction. The criteria that score an AUC
 243 value less than 0.5 have an indirect correlation with the wildfire records. The first two columns of Table 1
 244 present the absolute and normalized AUC values of all criteria.

245 **Table 1.** The weighted impact factors (WIPI and WSCI) of each criterion via AHP and ROC/AUC methods.

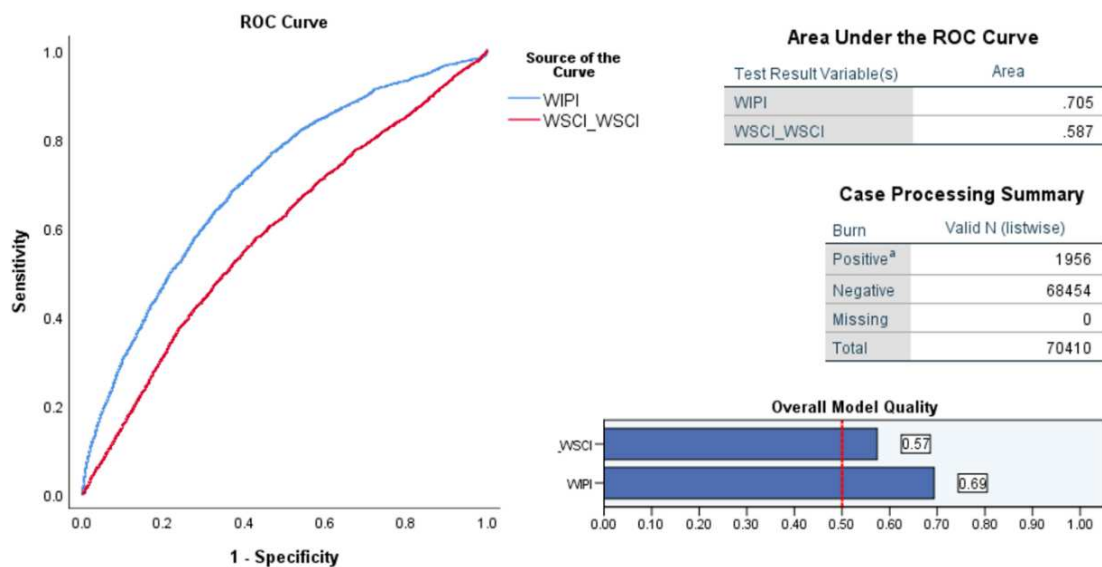
		WIPI				WSCI					
		ROC/ AUC	AUC/ norm	+ -	AHP	ROC	AUC/ norm	+ -	AHP	ROC	AUC/ norm
E1	Solar radiation	.823	.110	+	.032	.823	.110	+	.011	.823	.103
E2	Precipitation	.201	.027	-	.097	.799	.107	-	.048	.799	.100
E3	Max. Temp.	.811	.109	+	.032	.811	.108	+	.022	.811	.101
E4	Wind speed	.575	.077					+	.155	.575	.072
F1	Fuel type	.593	.080	+	.056	.593	.079	+	.033	.593	.074
F2	TCD	.388	.052					+	.299	.388	.048
F3	NDVI	.405	.054	-	.125	.405	.054	-	.170	.595	.074
P1	Slope	.278	.037					+	.033	.278	.035
P2	Aspect	.511	.069	+	.049	.511	.068	+	.013	.511	.064
P3	Altitude	.192	.026	-	.016	.808	.108	-	.006	.808	.101
P4	Dist. To water	.411	.055					+	.070	.411	.051
S1	Pop. density	.501	.067	+	.026	.499	.067				
S2	Dist. Settlements	.381	.051	-	.076	.619	.083	+	.017	.381	.048
S3	Dist. roads	.551	.074	-	.140	.449	.060	+	.006	.551	.069
S4	Dist. main roads	.477	.064	-	.045	.523	.070	+	.047	.477	.060
S5	Dist. agriculture	.354	.048	-	.305	.646	.086				

246 The following columns deliver each criterion's relative impact factors as calculated via AHP pairwise
 247 comparison and ROC/AUC analysis. Besides, each criterion is assigned an indicator for either direct (+) or
 248 inverse (-) relation with the wildfire risk. This indicator is assigned based on assumptions inferred from the
 249 literature review on the relationship between wildfire regimes and driving factors ¹⁹. For example, the highest
 250 the solar radiation, maximum temperature, fuel type, and aspect values, the wildfire ignition and spread the
 251

252 risk. On the other side, the lower the precipitation, NDVI, and altitude values, the higher the wildfire risk.
 253 Simultaneously, anthropogenic criteria like distance to settlements and transportation networks are unevenly
 254 related to wildfire ignition and spreading phases.

255 *3.3. Comparing between WIPI/ WSCI and WIPI_ROC/ WSCI_ROC Results*

256 We calculated the WIPI and WSCI index values of each reference point according to Eq. 1 and Eq. 2
 257 using the weighted values via the AHP method. The results of the ROC/AUC analysis show the relatively low
 258 sensitivity of the model. According to Fig. 5, the AUC of WIPI is 0.705 and an overall model quality of 0.69.
 259 It is significantly higher than the WSCI model sensitivity marking an AUC value of 0.587 and an overall
 260 model quality of 0.57. It can be inferred that the model, which relies on the weighted values calculated via
 261 AHP, is more accurate for predicting wildfire occurrence events rather than the wildfire spreading process.



262 **Figure 5.** Sensitivity analysis of the WIPI and WSCI models based on burned surfaces (2015-2019) as positive
 263 cases (1956 out of 70410-point locations).
 264

265
 266 Later, we recalculated each reference point's index values as the sum of the products between normalized
 267 inventory value and the weighted factor via the ROC/AUC method (Fig. 2). The revised weights, as presented
 268 in Table 1, led to improved model sensitivity. Fig. 6 presents a comparative ROC/AUC analysis between the
 269 former WIPI/WSCI and the revised WIPI_ROC/ WSCI_ROC models.

270 The updated models' curves are shown in green color, while the previous versions are shown in red.

271 According to Fig.6a, the AUC value of WIPI_ROC has jumped to 0.778, marking a sensitivity increase of

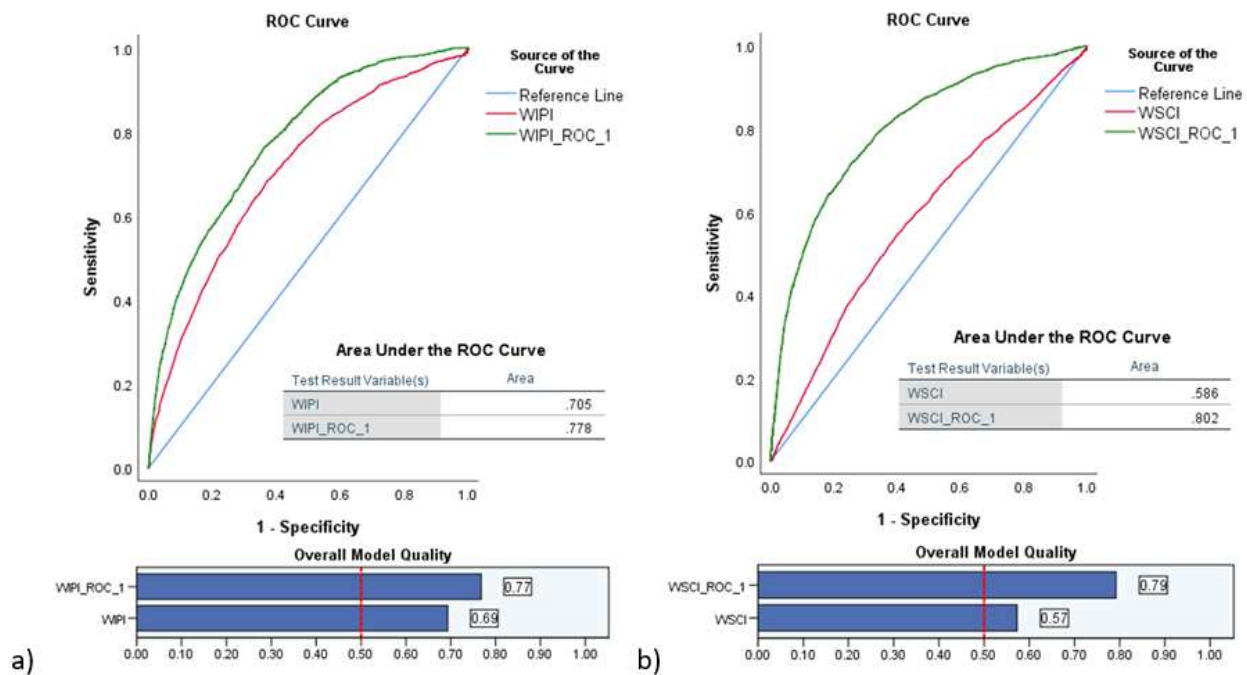
272 0.073. The overall model quality of the WIPI model has been improved by 12% (from 0.69 to 0.77). The

273 improvement is more visible in the case of the WSCI model (Fig. 6b). The revised model (WSCI_ROC)

274 records an AUC value of 0.802, 37% higher than the earlier version. A similar escalation is recognized in the

275 overall model quality. We rely on the WSCI_ROC results during the final stage of vulnerability and exposure

276 analysis.



277 **Figure 6.** Comparative Sensitivity analysis; (a) between WIPI and WIPI_ROC models, and (b) between WSCI

278 and WSCI_ROC models.

279

280

281 Beyond statistical analysis about the model accuracy, the results of the WSCI_ROC model delivers

282 essential findings of the spatial distribution of the wildfire spreading the capacity risk of vegetated surfaces in

283 Romania. According to Fig. 7, the highest wildfire spreading risk is concentrated in its eastern and southern

284 regions. A secondary area under wildfire spreading capacity risk is along the western borders. Simultaneously,

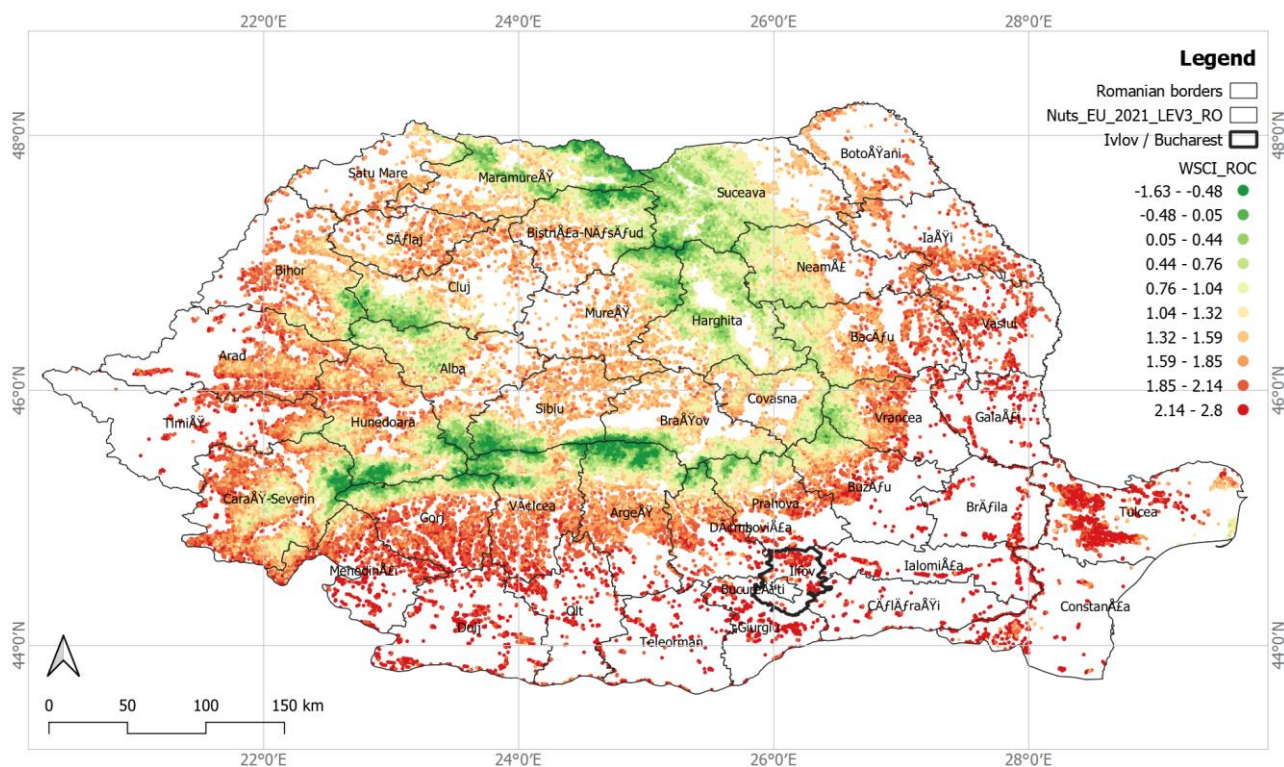
285 the central and the northern regions appear to be safer from wildfire, spreading the risk. These regions coincide

286 with the surfaces which are high in elevation and located away from human activities. Among them, the sub-

287 regions that record the lowest WSCI_ROC values are surfaces that are oriented towards the northern direction

288 and gaining a minimum of solar radiation. The gradient of green color indicates these surfaces.

289 Furthermore, Fig.7 includes the administrative boundaries of the third level (NUTS-L3) of Romania.
 290 Referring to the Eurostat data, Romania has 42 local administrative units at the third level. According to the
 291 results presented in Fig. 7 and Fig. S3 (see Supplementary file online), 41 units consist of at least 1km² of
 292 vegetated surface that has been indexed here. The only unit that has no wildland vegetated surface is the capital
 293 city of Romania. As highlighted in Fig. 7, Bucharest is the smallest in surface area compared to the other units.
 294 However, it does not mean that it is safer. On the contrary, when jointly considered with the metropolitan area
 295 of Ilfov, which envelopes the urban area of Bucharest, the wildfire ignition and spreading risk in the wildland-
 296 urban interface (WUI). We further discuss this issue in the following sections while assessing human-made
 297 structures' exposure to wildfire spreading risk.



298
 299 **Figure 7.** Wildfire spreading capacity map of vegetated surfaces on Romania (WSCI_ROC) with the
 300 highlighted metropolitan area of Ilfov.

301 The overlapping of wildfire spreading capacity risk and the local administrative units highlights the
 302 municipalities that need to enhance their wildfire prevention measures. Fig. S3 (Supplementary files online)
 303 presents the box plots that show the WIPI_ROC and WSCI_ROC values distribution by local administrative
 304 units. According to the results plotted in Fig. S3a, the administrative units with the highest WIPI_ROC index
 305 values are located in the country's south-eastern and southern regions.

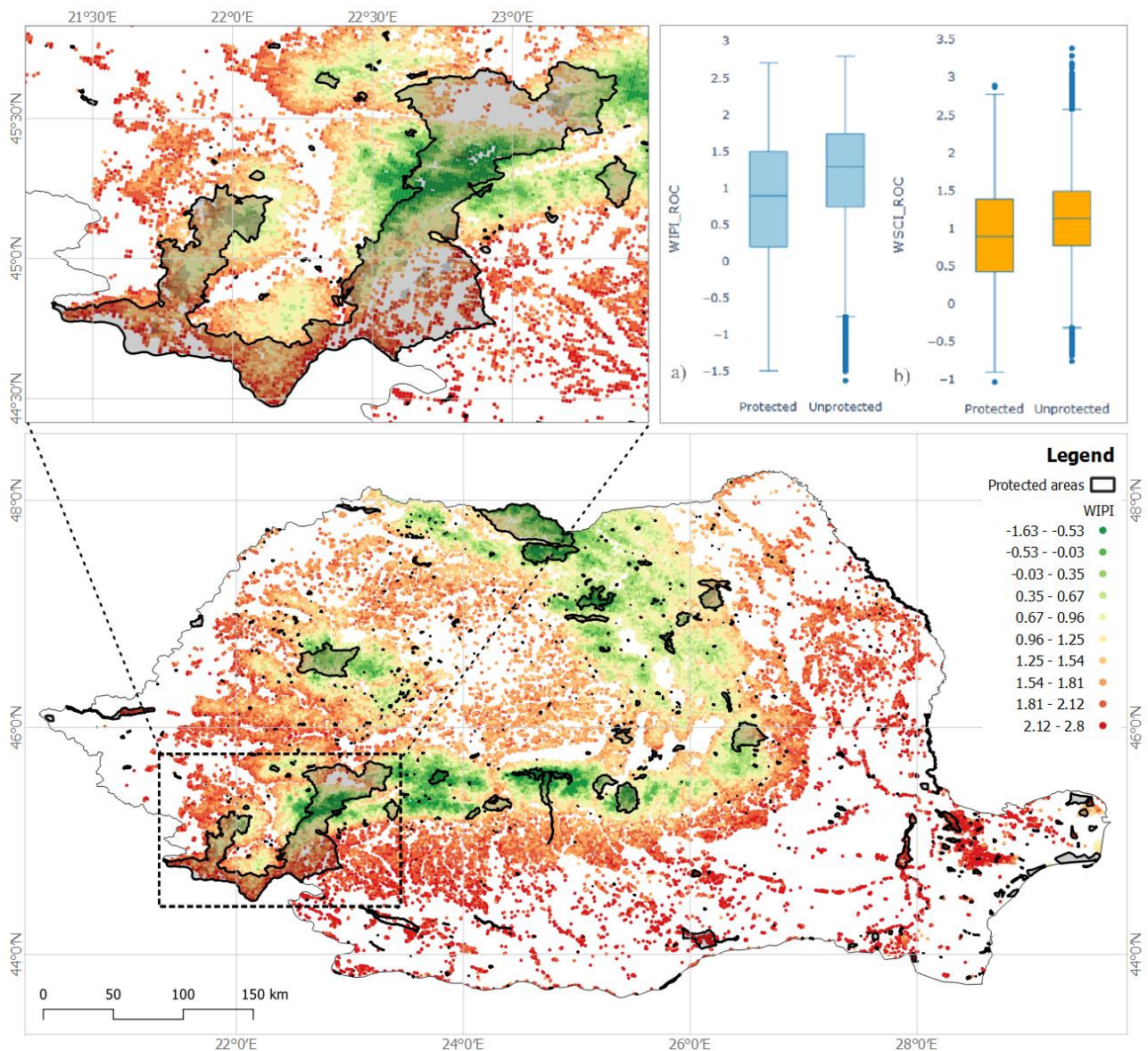
306 4. Discussions on Vulnerability and Exposure analysis

307 Wildfires are native events on earth estimated to have been happening during the last 350 million years
308 ³⁸. They are accepted to significantly contribute to vegetation recovery at their natural schedule, the
309 biogeochemical cycles of carbon and nitrogen, and the atmosphere's chemical properties ³⁹⁻⁴¹. However, they
310 are also reported to have considerable consequences on the territory's ecological and social systems. Protected
311 areas are among the land surfaces where the ecological and socio-cultural interests converge with each other.
312 Uncontrolled fires in the vegetated protected areas may cause unrecoverable consequences on the native
313 vegetation structure. On the other side, the WUI zone is boldly highlighted in scientific reports. Wildfire events
314 threaten human activities. We expand our findings by discussing further concerning protected areas'
315 vulnerability and exposure to human-made structures.

316 *4.1. The vulnerability of the Romanian Protected areas to Wildfires*

317 Globally speaking, the protected areas are under consistent threat caused by the processes of climate
318 change, land-use alterations, provisioning of raw materials, socio-cultural activities, and flourishing of
319 invasive species ^{42,43}. Jones et al. ⁴⁴ conclude that only two-thirds of the protected areas are safe from globally
320 intensive human activities. While Schulze et al. ⁴⁵ list fire and fire suppression activities as the third out of 36
321 threats that protected areas usually face according to the list of level two threats included in the IUCN-CMP
322 Threats Classification Scheme. Forest fires can lead to an invasive plant expansion in disturbed sites ⁴⁶. The
323 native species in Romania's protected areas have been at risk of several natural and human-induced hazards
324 ⁴⁷. Thus, assessing the vulnerability of the protected areas to wildfires is of great concern in Romania.

325 This assessment relies on the European inventory of nationally designated protected areas, as acquired
326 from the EEA open-source datasets. According to these data, Romania has 946 protected sites, covering a total
327 area of 13985 km². Fig. 8 presents the protected areas overlapping the WIPI_ROC results. Most of these areas
328 are found in the alpine lands along with the RCM. About 13% of the 70410 reference points within the
329 vegetated surfaces we analyzed are located within the protected areas. Consequently, we may infer that 65%
330 of Romania's protected surfaces are vegetated and potentially vulnerable to wildfire risk.



331 **Figure 8.** Wildfire spreading risk exposure map of protected areas in Romania, and comparative box plot of
 332 WIPI_ROC (a) and WSCI_ROC (b) value distribution between protected and unprotected vegetated surfaces
 333 in Romania.
 334

335

336 According to the box plot in Fig. 8a-b, the protected areas have lower WIPI_ROC and WSCI_ROC values
 337 than unprotected surfaces. Furthermore, referring to Fig. 8, most vegetated surfaces within the protected
 338 patches are greenish, implying a relatively low wildfire spreading capacity (WSCI_ROC). These values' main
 339 reasons are the high elevation and remote location of protected surfaces to human activities (settlement and
 340 transportation network). However, some cases consist of a gradient of WSCI_ROC values within the same
 341 protected surface (see the enlarged protected patch in Fig. 8).

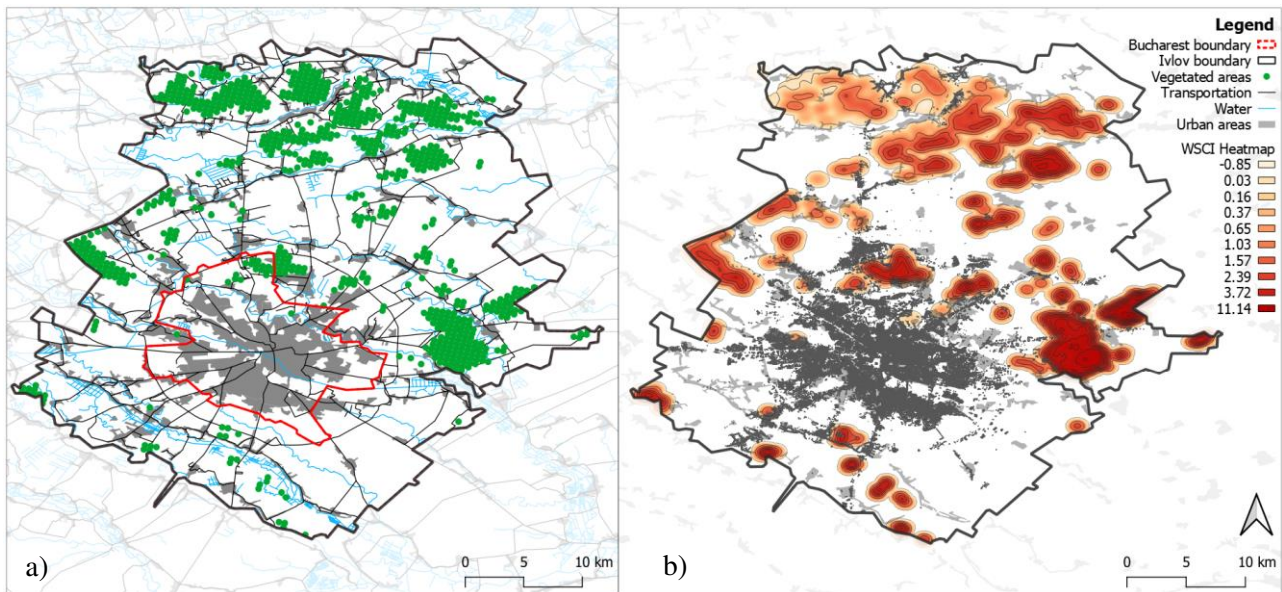
342 The relation between connectivity among vegetated landscape patches and wildfire spreading risk has
343 been a questionable literature topic ⁴⁸. O'Donnell et al. ⁴⁹ report that the fragmentation among vegetated
344 landscapes in unmanaged Australian semi-arid shrublands and woodlands directly impacts the reduction of
345 wildfire intervals between 1940 and 2006. Thus, the connectivity among vegetated surfaces within the same
346 protected area may boost the wildfire, spreading greenish areas' risk. Future studies must focus on specifically
347 protected patches to assess the vulnerability to wildfire spreading risk at a finer spatial scale.

348 *4.2. Wildfire exposure of populated areas within the metropolitan area of Bucharest*

349 The urban fringes are critical hybrid areas where the human-made structures are exposed to different
350 environmental hazards ⁵⁰. Studies from developing countries report that uncontrolled urban expansion
351 increases inhabited surfaces' exposure to natural hazards like floods, landslides, fire, and sinkholes, among
352 others ⁵¹. Sestras et al. ⁵² report landslide assessment at a local scale as an inherent threat in Romania's newly
353 developed suburban zones. The wildland-urban interface represents an area of contradiction where both the
354 settling interest and wildfire risk are significantly high ^{53,54}.

355 We performed an exposure assessment of built structures to the wildfire spreading capacity of vegetated
356 surfaces within the Romanian capital city's metropolitan area (Fig. 9a). The wildfire exposure analysis relies
357 on the juxtaposition between the WSCI_ROC results and existing building stock, as shown in Fig. 9. We bring
358 a demonstrative example from Ilfov metropolitan area, which includes the capital city, Bucharest. The hazard
359 map of wildfire spreading capacity relies on the results reported in this article (see Fig. 7). The WSCI_ROC
360 point's layer is utilized for preparing the hazard heatmap (kernel density estimation) with a selection radius of
361 1km.

362



363

364

365

Figure 9. Wildfire exposure map of existing urban fabric (b) within Ilfov and Bucharest (a), and box plot of WSCI_cum distribution per building type of exposed structures (c).

366

367

368

369

370

371

OSM data provide the building stock within the focal study area. Nevertheless, OSM data accuracy is still debatable due to the lack of professional backgrounds⁵⁵. A substantial number of building features that do not include building-use information. However, we bring this discussion as an exposure analysis method that can deliver critical information about the human-made structures under wildfire risk within WUI areas at a metropolitan scale if further improved by introducing validated building stock data.

372

373

According to Fig. 9b, 9596 structures overlap with the WSCI_ROC heatmap, exposing the minimum wildfire spreading capacity. Furthermore, 1734 out of the total exposed structures are building types of

374 significant socio-economic. This building stock's exposure to wildfire spreading risk may have critical
375 consequences on socio-economical processes and their users' life security. Fig. 9c presents the box plot of
376 WSCI_ROC heatmap values distribution per building type. We have included just the most critical building
377 types like hospitals, industrial, residential, religious, leisure, and educational use. While other buildings like
378 warehouses, greenhouses, and abandoned structures, have been ignored at this stage.

379 According to the box plot, just one hospital is located within the critical wildfire spreading capacity
380 heatmap. Nevertheless, it has a WSCI_ROC heatmap value of 2.37, which indicates a significant exposure of
381 its users to wildfire spreading risk. According to the outlier values (dots) shown in Fig. 9c, there are four
382 industrial, one house, and one school building highly exposed to wildfire spreading the risk.

383 **5. Conclusions**

384 This study presented the indexing of vegetated surfaces in Romania by Wildfire Ignition Probability and
385 Spreading Capacity Index (WIPI/ WSCI). The method offered here relies on open-source data, which supplies
386 the analytical process with geospatial information about the anthropogenic, hydro-meteorological,
387 geophysical, and fuel properties of the study area. We identified sixteen criteria that significantly impact either
388 the wildfire ignition or spreading phase of the wildfire event in Romania. Nevertheless, the impact of each
389 criterion on wildfire is weighted via ROC/ AUC analysis. During the analysis, the positive cases rely on the
390 burned area fraction records between 2015 and 2019 (five years).

391 According to the results, the hydro-meteorological criteria have the highest correlation with the wildfire
392 records. The vegetated surfaces in Romania's eastern and southern regions face the highest wildfire spreading
393 capacity index values. Considering that these regions make home to urbanized lands of high population
394 density, the high WSCI records indicate an elevated risk. We performed the wildfire spreading risk exposure
395 analysis of the building stock within the capital city's metropolitan area, Bucharest. These results imply that
396 critical structures like hospitals, residential and educational units are at significant risk.

397 On the other side, Romania's central areas scattered along the RCM have the lowest index values. This is
398 generally driven by high altitude values, directly correlated with other climatic criteria such as solar radiation,
399 precipitation, and maximum temperature. These regions include the majority of protected areas. According to

400 our results, some protected vegetated surfaces in Romania hold a gradient of wildfire spreading risk within
401 the same protected area geometry. In such cases, the whole area within the protection borders must be
402 considered under risk as the connectivity among vegetated surfaces in wildfire risk analysis is considered a
403 weakness.

404 The method we presented in this study is reproducible in other wildfire-prone geographies. It is also
405 flexible enough to integrate the most up-to-date and the most reliable remotely sensed geospatial data. The
406 results presented in this study can help the institutions at the national and local levels responsible for wildfire
407 risk reduction in Romania.

408 **Data availability**

409 The data generated during this study are included in this published article are shared via the PANGAEA
410 database and can be accessed via the following link. <https://issues.pangaea.de/browse/PDI-27019>

411 **References**

- 412
- 413 1 AghaKouchak, A. *et al.* How do natural hazards cascade to cause disasters? *Nature* **561**, 458-460,
414 doi:<https://doi.org/10.1038/d41586-018-06783-6> (2018).
- 415 2 Naderpour, M. & Khakzad, N. Texas LPG fire: Domino effects triggered by natural hazards. *Process Safety and*
416 *Environmental Protection* **116**, 354-364, doi:<https://doi.org/10.1016/j.psep.2018.03.008> (2018).
- 417 3 Ruffault, J. *et al.* Increased likelihood of heat-induced large wildfires in the Mediterranean Basin. *Scientific Reports*
418 **10**, 13790, doi:10.1038/s41598-020-70069-z (2020).
- 419 4 Chapin, F. S. *et al.* Increasing Wildfire in Alaska's Boreal Forest: Pathways to Potential Solutions of a Wicked
420 Problem. *BioScience* **58**, 531-540, doi:10.1641/B580609 %J BioScience (2008).
- 421 5 Levin, N., Tessler, N., Smith, A. & McAlpine, C. The Human and Physical Determinants of Wildfires and Burnt
422 Areas in Israel. *Environmental Management* **58**, 549-562, doi:10.1007/s00267-016-0715-1 (2016).
- 423 6 Ganteaume, A. *et al.* A Review of the Main Driving Factors of Forest Fire Ignition Over Europe. *Environmental*
424 *Management* **51**, 651-662, doi:10.1007/s00267-012-9961-z (2013).
- 425 7 Guo, F. *et al.* Wildfire ignition in the forests of southeast China: Identifying drivers and spatial distribution to
426 predict wildfire likelihood. *Applied Geography* **66**, 12-21, doi:<https://doi.org/10.1016/j.apgeog.2015.11.014> (2016).
- 427 8 Ruffault, J. & Mouillot, F. Contribution of human and biophysical factors to the spatial distribution of forest fire
428 ignitions and large wildfires in a French Mediterranean region %J International Journal of Wildland Fire. **26**,
429 498-508, doi:<https://doi.org/10.1071/WF16181> (2017).
- 430 9 Davis, R., Yang, Z., Yost, A., Belongie, C. & Cohen, W. The normal fire environment—Modeling environmental
431 suitability for large forest wildfires using past, present, and future climate normals. *Forest Ecology and Management*
432 **390**, 173-186, doi:<https://doi.org/10.1016/j.foreco.2017.01.027> (2017).
- 433 10 Granström, A. Spatial and temporal variation in lightning ignitions in Sweden. *Journal of Vegetation Science* **4**, 737-
434 744, doi:<https://doi.org/10.2307/3235609> (1993).
- 435 11 Curt, T., Fréjaville, T. & Lahaye, S. Modelling the spatial patterns of ignition causes and fire regime features in
436 southern France: implications for fire prevention policy %J International Journal of Wildland Fire. **25**, 785-796,
437 doi:<https://doi.org/10.1071/WF15205> (2016).
- 438 12 Hawbaker, T. J. *et al.* Human and biophysical influences on fire occurrence in the United States. *Ecological*
439 *Applications* **23**, 565-582, doi:<https://doi.org/10.1890/12-1816.1> (2013).
- 440 13 Mahmoud, H. & Chulahwat, A. Unraveling the Complexity of Wildland Urban Interface Fires. *Scientific Reports*
441 **8**, 9315, doi:10.1038/s41598-018-27215-5 (2018).
- 442 14 Mansuy, N. *et al.* Contrasting human influences and macro-environmental factors on fire activity inside and
443 outside protected areas of North America. *Environmental Research Letters* **14**, 064007, doi:10.1088/1748-
444 9326/ab1bc5 (2019).
- 445 15 Syphard, A. D., Keeley, J. E., Pfaff, A. H. & Ferschweiler, K. Human presence diminishes the importance of
446 climate in driving fire activity across the United States. **114**, 13750-13755, doi:10.1073/pnas.1713885114 %J
447 Proceedings of the National Academy of Sciences (2017).
- 448 16 Kountouris, Y. Human activity, daylight saving time and wildfire occurrence. *Science of The Total Environment*
449 **727**, 138044, doi:<https://doi.org/10.1016/j.scitotenv.2020.138044> (2020).
- 450 17 Rodrigues, M., Gelabert, P. J., Ameztegui, A., Coll, L. & Vega-García, C. Has COVID-19 halted winter-spring
451 wildfires in the Mediterranean? Insights for wildfire science under a pandemic context. *Science of The Total*
452 *Environment* **765**, 142793, doi:<https://doi.org/10.1016/j.scitotenv.2020.142793> (2021).

- 453 18 Mann, M. L. *et al.* Incorporating Anthropogenic Influences into Fire Probability Models: Effects of Human
454 Activity and Climate Change on Fire Activity in California. *PLOS ONE* **11**, e0153589,
455 doi:10.1371/journal.pone.0153589 (2016).
- 456 19 Hysa, A. & Bařkaya, F. A. T. A GIS based method for indexing the broad-leaved forest surfaces by their wildfire
457 ignition probability and wildfire spreading capacity. *Modeling Earth Systems and Environment* **5**, 71-84,
458 doi:10.1007/s40808-018-0519-9 (2019).
- 459 20 Hysa, A. & Teqja, Z. Counting fuel properties as input in the wildfire spreading capacities of vegetated surfaces:
460 case of Albania. *Notulae Botanicae Horti Agrobotanici Cluj-Napoca* **48**, 1667-1682, doi:10.15835/nbha48311994 (2020).
- 461 21 Adámek, M., Jankovská, Z., Hadincová, V., Kula, E. & Wild, J. Drivers of forest fire occurrence in the cultural
462 landscape of Central Europe. *Landscape Ecology* **33**, 2031-2045, doi:10.1007/s10980-018-0712-2 (2018).
- 463 22 Pinto, G. A. S. J., Rousseu, F., Niklasson, M. & Drobyshev, I. Effects of human-related and biotic landscape
464 features on the occurrence and size of modern forest fires in Sweden. *Agricultural and Forest Meteorology* **291**,
465 108084, doi:<https://doi.org/10.1016/j.agrformet.2020.108084> (2020).
- 466 23 Ioja, C. I., Grădinaru, S. R., Onose, D. A., Vânău, G. O. & Tudor, A. C. The potential of school green areas to
467 improve urban green connectivity and multifunctionality. *Urban Forestry & Urban Greening* **13**, 704-713,
468 doi:<https://doi.org/10.1016/j.ufug.2014.07.002> (2014).
- 469 24 Dumitrașcu, M. *et al.* Estimation of Future Changes in Aboveground Forest Carbon Stock in Romania. A
470 Prediction Based on Forest-Cover Pattern Scenario. *Forests* **11**, 914 (2020).
- 471 25 Popovici, E. A., Bălțeanu, D., Kucsicsa, G. J. C. J. o. E. & Sciences, E. Assessment of changes in land-use and land-
472 cover pattern in Romania using Corine Land Cover Database. **8**, 195-208 (2013).
- 473 26 Kucsicsa, G. *et al.* Assessing the Potential Future Forest-Cover Change in Romania, Predicted Using a Scenario-
474 Based Modelling. *Environmental Modeling & Assessment* **25**, 471-491, doi:10.1007/s10666-019-09686-6 (2020).
- 475 27 Munteanu, C., Nita, M. D., Abrudan, I. V. & Radeloff, V. C. Historical forest management in Romania is imposing
476 strong legacies on contemporary forests and their management. *Forest Ecology and Management* **361**, 179-193,
477 doi:<https://doi.org/10.1016/j.foreco.2015.11.023> (2016).
- 478 28 Hysa, A. & Spalevic, V. Testing NDVI, tree cover density and land cover type as fuel indicators in the wildfire
479 spread capacity index (WSCI): case of Montenegro. *Notulae Botanicae Horti Agrobotanici Cluj-Napoca* **48**, 2368-2384,
480 doi:10.15835/nbha48411993 (2020).
- 481 29 Jain, A., Nandakumar, K. & Ross, A. Score normalization in multimodal biometric systems. *Pattern Recognition*
482 **38**, 2270-2285, doi:<https://doi.org/10.1016/j.patcog.2005.01.012> (2005).
- 483 30 Büttner, G. & Kosztra, B. 1-60 (2017).
- 484 31 Didan, K. J. N. E. L. P. D. MOD13Q1 MODIS/Terra vegetation indices 16-day L3 global 250m SIN grid V006. **10**
485 (2015).
- 486 32 Palchaudhuri, M. & Biswas, S. Application of LISS III and MODIS-derived vegetation indices for assessment of
487 micro-level agricultural drought. *The Egyptian Journal of Remote Sensing and Space Science* **23**, 221-229,
488 doi:<https://doi.org/10.1016/j.ejrs.2019.12.004> (2020).
- 489 33 Fick, S. E. & Hijmans, R. J. WorldClim 2: new 1-km spatial resolution climate surfaces for global land areas.
490 *International Journal of Climatology* **37**, 4302-4315, doi:<https://doi.org/10.1002/joc.5086> (2017).
- 491 34 Buontempo, C. *et al.* Fostering the development of climate services through Copernicus Climate Change Service
492 (C3S) for agriculture applications. *Weather and Climate Extremes* **27**, 100226,
493 doi:<https://doi.org/10.1016/j.wace.2019.100226> (2020).

- 494 35 Loepfe, L., Lloret, F. & Román-Cuesta, R. M. Comparison of burnt area estimates derived from satellite products
495 and national statistics in Europe. *International Journal of Remote Sensing* **33**, 3653-3671,
496 doi:10.1080/01431161.2011.631950 (2012).
- 497 36 Giglio, L., van der Werf, G. R., Randerson, J. T., Collatz, G. J. & Kasibhatla, P. Global estimation of burned area
498 using MODIS active fire observations. *Atmos. Chem. Phys.* **6**, 957-974, doi:10.5194/acp-6-957-2006 (2006).
- 499 37 Mouillot, F. *et al.* Ten years of global burned area products from spaceborne remote sensing—A review: Analysis
500 of user needs and recommendations for future developments. *International Journal of Applied Earth Observation*
501 *and Geoinformation* **26**, 64-79, doi:<https://doi.org/10.1016/j.jag.2013.05.014> (2014).
- 502 38 He, T., Belcher, C. M., Lamont, B. B. & Lim, S. L. A 350-million-year legacy of fire adaptation among conifers.
503 *Journal of Ecology* **104**, 352-363, doi:<https://doi.org/10.1111/1365-2745.12513> (2016).
- 504 39 Crisp, M. D., Burrows, G. E., Cook, L. G., Thornhill, A. H. & Bowman, D. M. J. S. Flammable biomes dominated
505 by eucalypts originated at the Cretaceous–Palaeogene boundary. *Nature Communications* **2**, 193,
506 doi:10.1038/ncomms1191 (2011).
- 507 40 Pausas, J. G. & Keeley, J. E. Abrupt Climate-Independent Fire Regime Changes. *Ecosystems* **17**, 1109-1120,
508 doi:10.1007/s10021-014-9773-5 (2014).
- 509 41 Zhu, C., Kobayashi, H., Kanaya, Y. & Saito, M. Size-dependent validation of MODIS MCD64A1 burned area over
510 six vegetation types in boreal Eurasia: Large underestimation in croplands. *Scientific Reports* **7**, 4181,
511 doi:10.1038/s41598-017-03739-0 (2017).
- 512 42 Radeloff, V. C. *et al.* Housing growth in and near United States protected areas limits their conservation value.
513 **107**, 940-945, doi:10.1073/pnas.0911131107 %J Proceedings of the National Academy of Sciences (2010).
- 514 43 Geldmann, J., Joppa, L. N. & Burgess, N. D. Mapping Change in Human Pressure Globally on Land and within
515 Protected Areas. *Conservation Biology* **28**, 1604-1616, doi:<https://doi.org/10.1111/cobi.12332> (2014).
- 516 44 Jones, K. R. *et al.* One-third of global protected land is under intense human pressure. **360**, 788-791,
517 doi:10.1126/science.aap9565 %J Science (2018).
- 518 45 Schulze, K. *et al.* An assessment of threats to terrestrial protected areas. *Conservation Letters* **11**, e12435,
519 doi:<https://doi.org/10.1111/conl.12435> (2018).
- 520 46 Ditomaso, J. M. *et al.* Control of Invasive Weeds with Prescribed Burning. *Weed Technology* **20**, 535-548,
521 doi:10.1614/WT-05-086R1.1 (2006).
- 522 47 Grigorescu, I., Kucsicsa, G., Dumitraşcu, M. & Doroftei, M. Invasive terrestrial plant species in the Romanian
523 protected areas. A review of the geographical aspects %J Folia Oecologica. **47**, 168-177,
524 doi:<https://doi.org/10.2478/foecol-2020-0020> (2020).
- 525 48 Martín-Martín, C., Bunce, R. G. H., Saura, S. & Elena-Rosselló, R. Changes and interactions between forest
526 landscape connectivity and burnt area in Spain. *Ecological Indicators* **33**, 129-138,
527 doi:<https://doi.org/10.1016/j.ecolind.2013.01.018> (2013).
- 528 49 O'Donnell, A. J., Boer, M. M., McCaw, W. L. & Grierson, P. F. Vegetation and landscape connectivity control
529 wildfire intervals in unmanaged semi-arid shrublands and woodlands in Australia. *Journal of Biogeography* **38**,
530 112-124, doi:<https://doi.org/10.1111/j.1365-2699.2010.02381.x> (2011).
- 531 50 Brenner, J. C. & Franklin, K. A. Living on the Edge: Emerging Environmental Hazards on the Peri-Urban Fringe.
532 *Environment: Science and Policy for Sustainable Development* **59**, 16-29, doi:10.1080/00139157.2017.1374793 (2017).
- 533 51 Rimal, B., Baral, H., Stork, N. E., Paudyal, K. & Rijal, S. Growing City and Rapid Land Use Transition: Assessing
534 Multiple Hazards and Risks in the Pokhara Valley, Nepal. *Land* **4**, 957-978 (2015).

- 535 52 Sestras, P. *et al.* Geodetic and UAV Monitoring in the Sustainable Management of Shallow Landslides and
536 Erosion of a Susceptible Urban Environment. *Remote Sensing* **13**, 385 (2021).
- 537 53 Davis, J. B. The wildland-urban interface: paradise or battleground? *Journal of Forestry* **88**, 26-31 (1990).
- 538 54 Hysa, A. in *Integrated Research on Disaster Risks: Contributions from the IRDR Young Scientists Programme* (eds
539 Riyanti Djalante, Mizan B. F. Bisri, & Rajib Shaw) 51-70 (Springer International Publishing, 2021).
- 540 55 Basiri, A. *et al.* Quality assessment of OpenStreetMap data using trajectory mining. *Geo-spatial Information Science*
541 **19**, 56-68, doi:10.1080/10095020.2016.1151213 (2016).
542

543 **ACKNOWLEDGMENTS**

544 The authors are thankful to the institutions that supplied the open-access data that we utilized in our work. We
545 acknowledge the use of data and/or imagery from NASA's Land, Atmosphere Near real-time Capability for
546 EOS (LANCE) system (<https://earthdata.nasa.gov/lance>), part of the NASA Earth Observing System Data and
547 Information System (EOSDIS).

548 **AUTHOR CONTRIBUTIONS STATEMENT**

549 **A.H.** Defined the methodology, acquired the materials, performed the GIS modeling, produced the visual
550 materials, wrote the draft manuscript. **V.S.** and **B.D.** Proposed the collaboration, supervised the study, acquired
551 the funding. **S.R.** Contributed to the manuscript, curated data, provided raw data. **A.K.** Supervised the study,
552 wrote and edited the final manuscript, curated the visual quality of figures. **Ş.B.** and **P.S.** Proposed the study,
553 wrote the original manuscript, curated data, supervised the study, provided raw data. All authors reviewed and
554 approved the manuscript.

555 **COMPETING INTERESTS**

556 The authors declare no competing interests

557 **ADDITIONAL INFORMATION**

558 **Supplementary Information** The online version contains supplementary material.

559 **Correspondence** and requests for materials should be addressed to A.H.

560

Figures

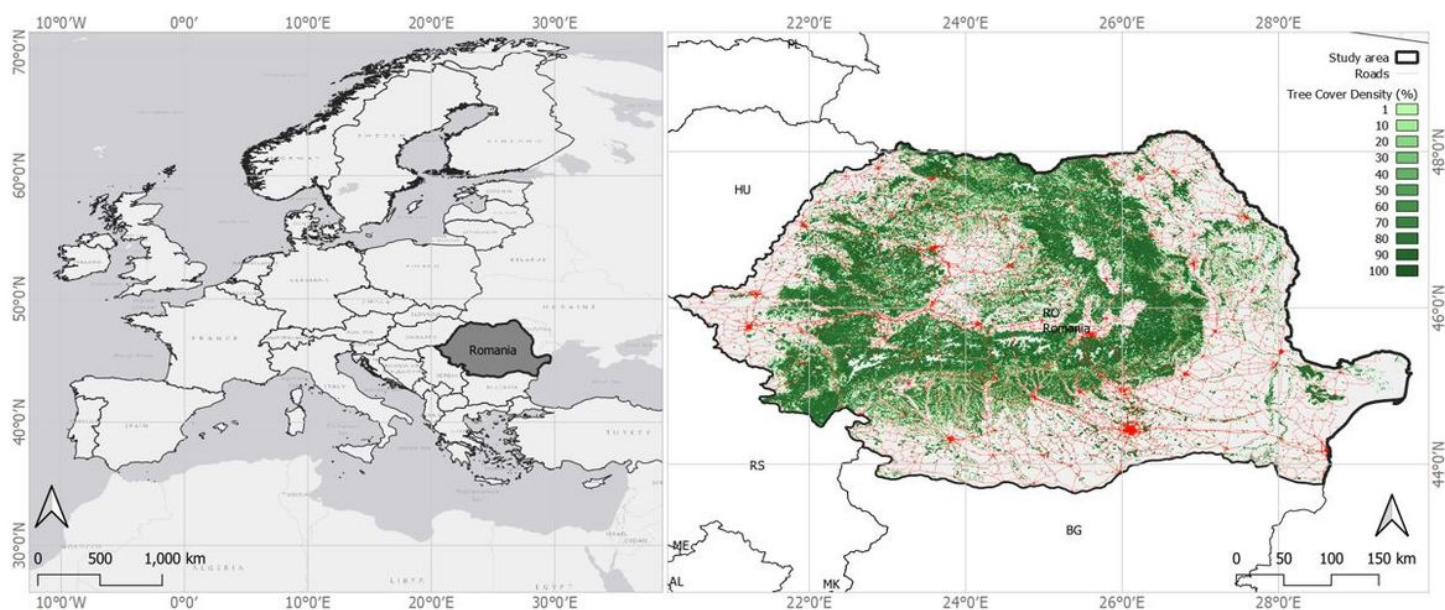


Figure 1

Romania within Europe (a), and Romanian territory including tree cover density (TCD) and transportation network distribution (b). Note: The designations employed and the presentation of the material on this map do not imply the expression of any opinion whatsoever on the part of Research Square concerning the legal status of any country, territory, city or area or of its authorities, or concerning the delimitation of its frontiers or boundaries. This map has been provided by the authors.

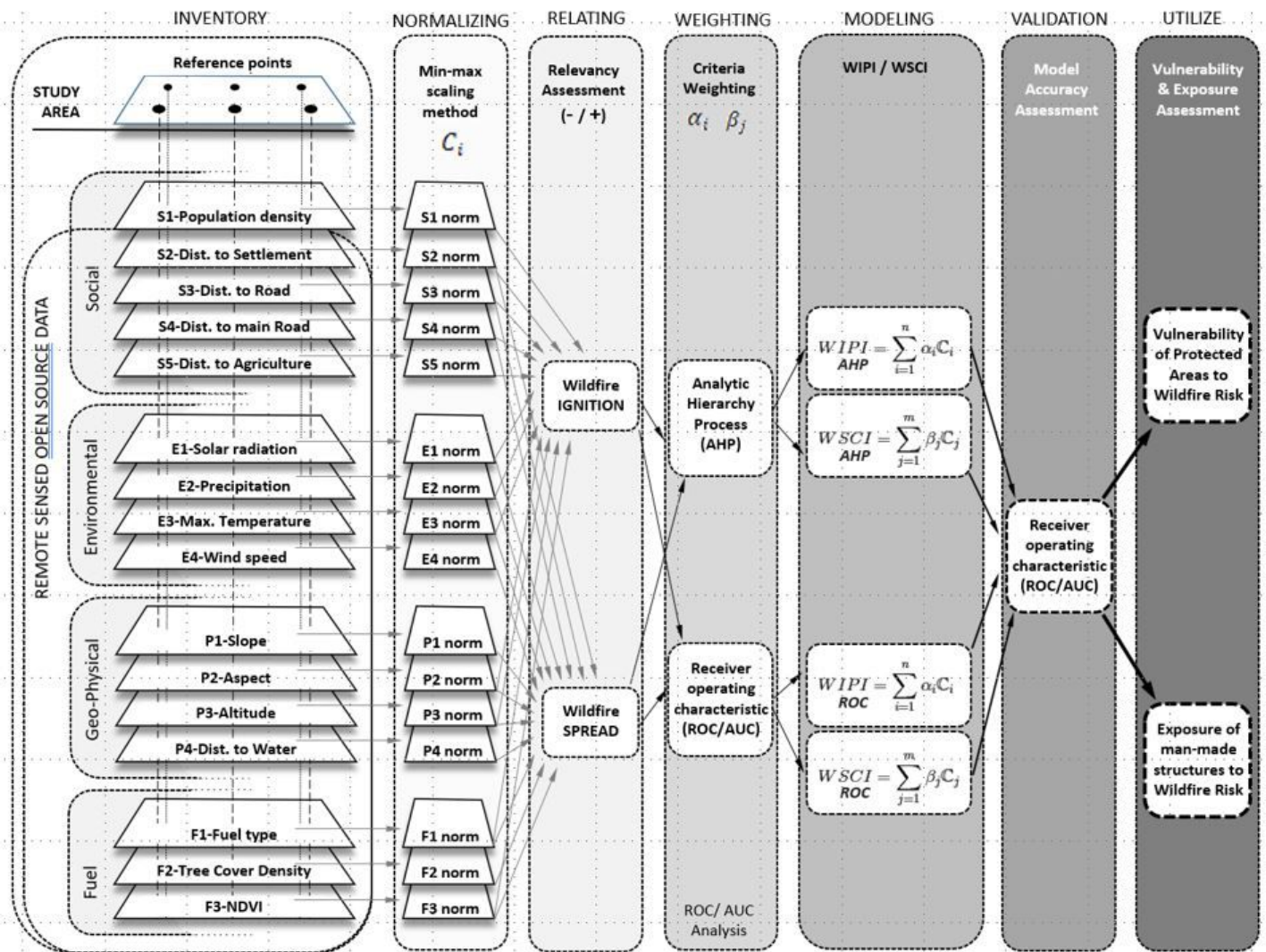


Figure 2

Workflow seven stages of the method.

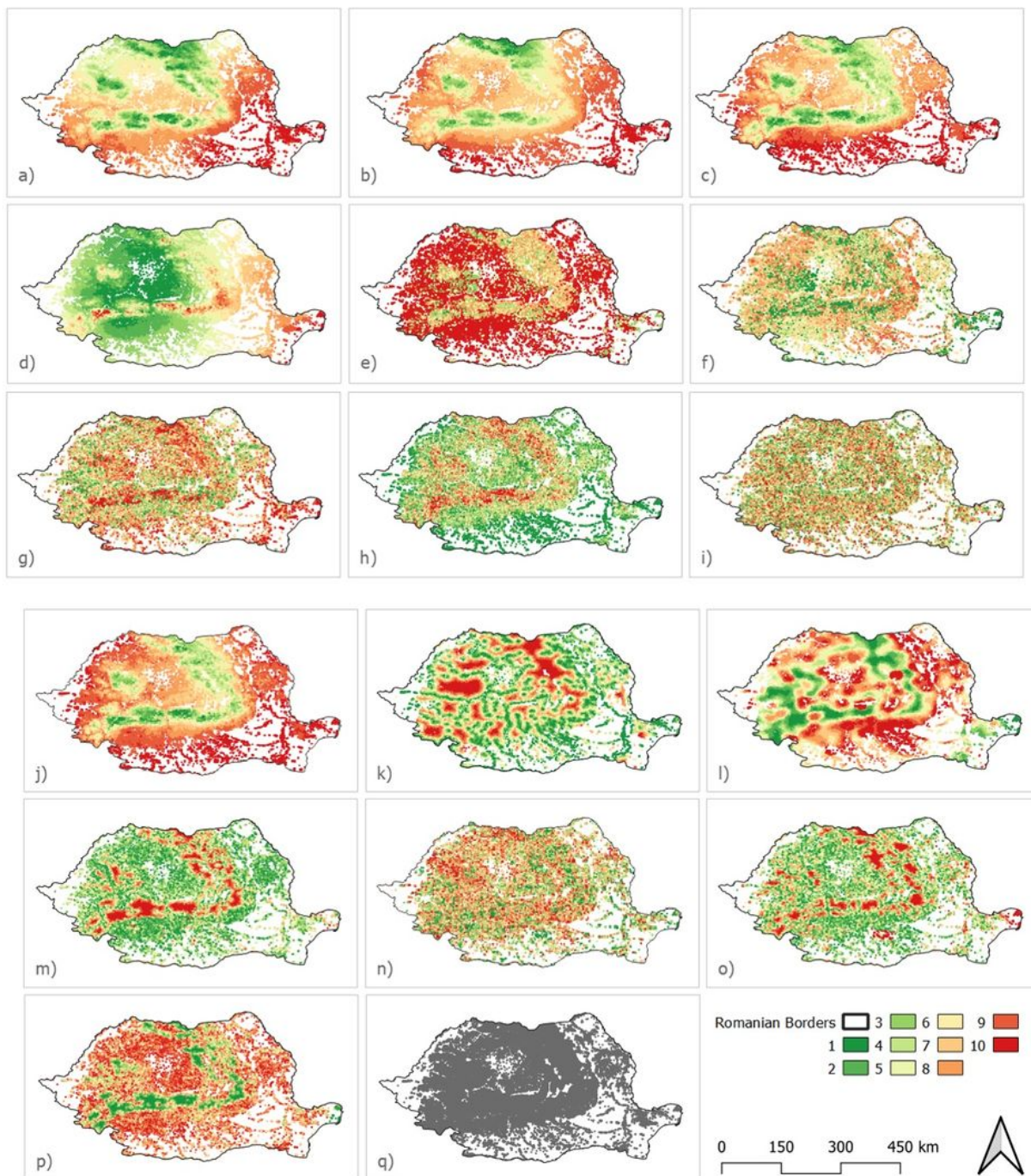


Figure 3

The relative risk of vegetated surfaces (q) in Romania for each criterion; (a) solar radiation, (b) precipitation, (c) maximum temperature, (d) wind speed, (e) fuel type, (f) tree cover density, (g) NDVI, (h) slope, (i) aspect, (j) altitude, (k) distance to water, (l) distance to urban centers, (m) distance to settlements, (n) distance to any road, (o) distance to main roads, (p) distance to agriculture. Note: The designations employed and the presentation of the material on this map do not imply the expression of

any opinion whatsoever on the part of Research Square concerning the legal status of any country, territory, city or area or of its authorities, or concerning the delimitation of its frontiers or boundaries. This map has been provided by the authors.

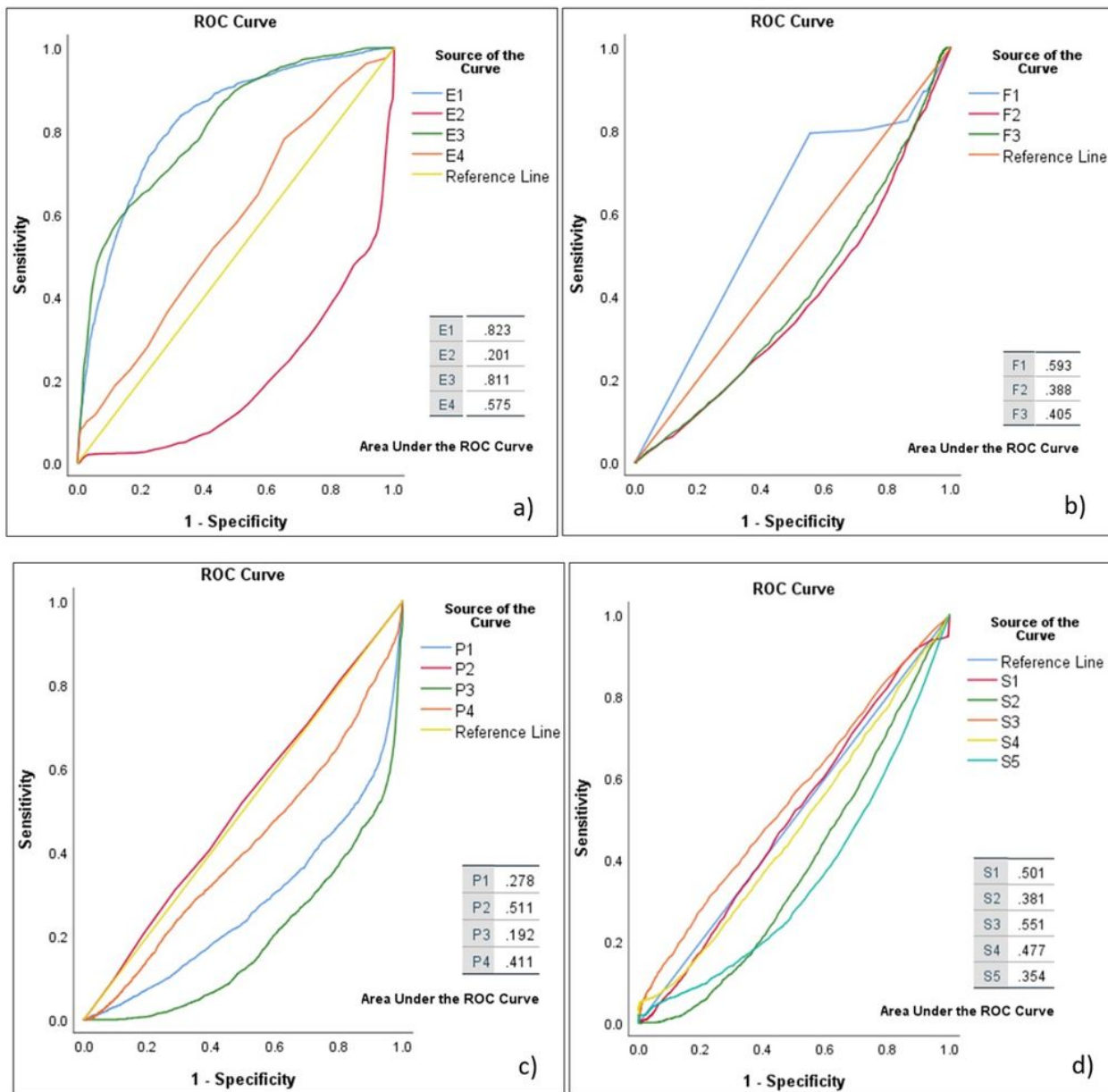


Figure 4

ROC curve analyses for (a) hydro-meteorological (E1-solar radiation, E2-precipitation, E3-maximum temperature, E4-wind speed), (b) fuel (F1-fuel type, F2-tree cover density, F3-ndvi), (c) geophysical (P1-slope, P2-aspect, P3-altitude, P4-distance to water), and (d) anthropogenic/ social (S1-population density,

S2-distance to settlements, S3-distance to any road, S4-distance to main roads) factors about burned regime values.

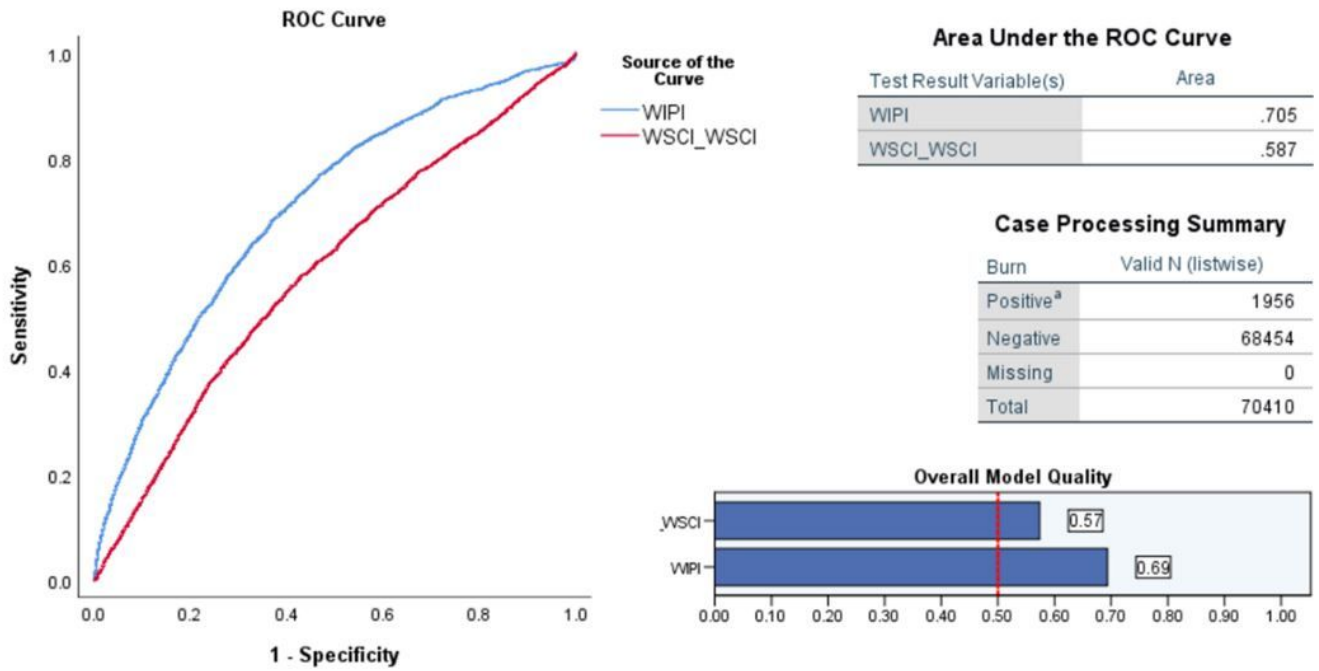


Figure 5

Sensitivity analysis of the WIPI and WSCI models based on burned surfaces (2015-2019) as positive cases (1956 out of 70410-point locations).

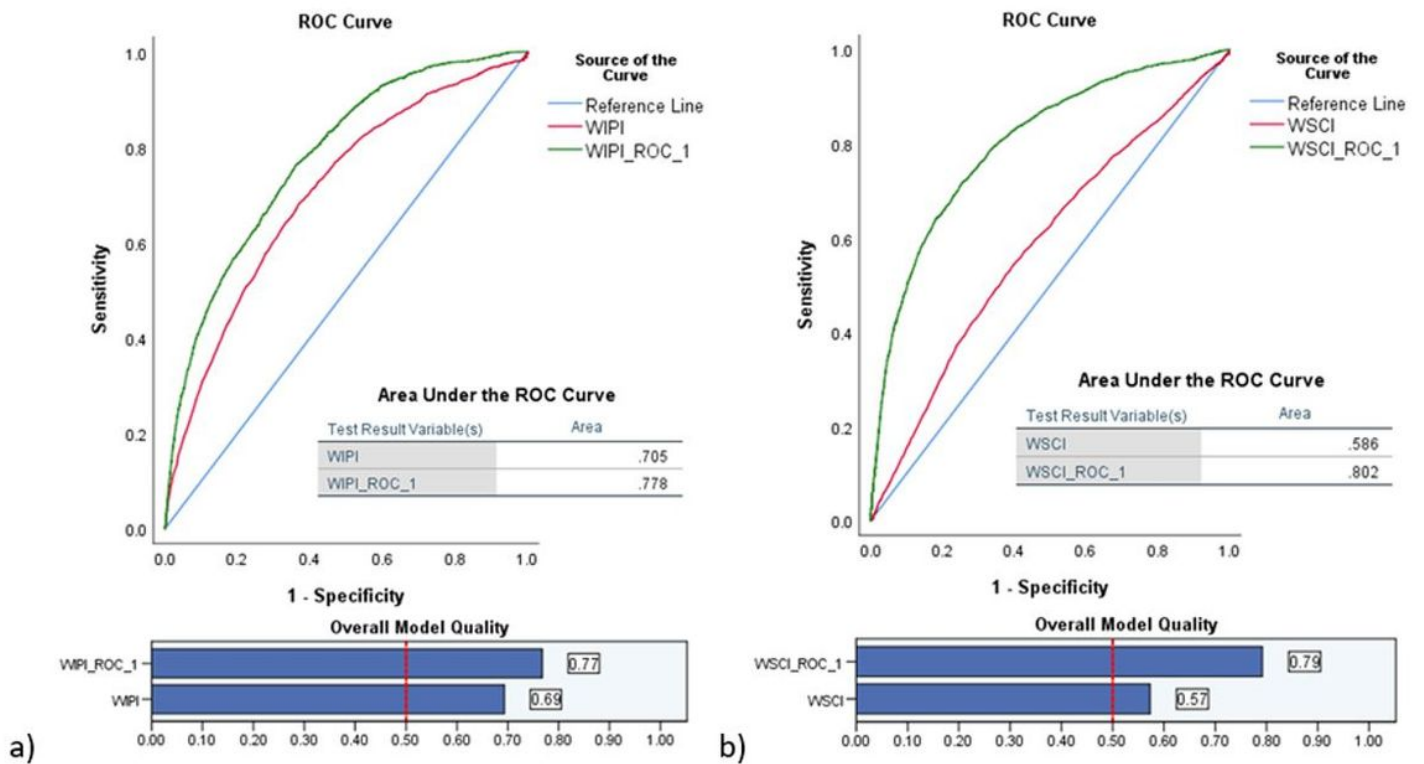


Figure 6

Comparative Sensitivity analysis; (a) between WIPI and WIPI_ROC models, and (b) between WSCI and WSCI_ROC models.

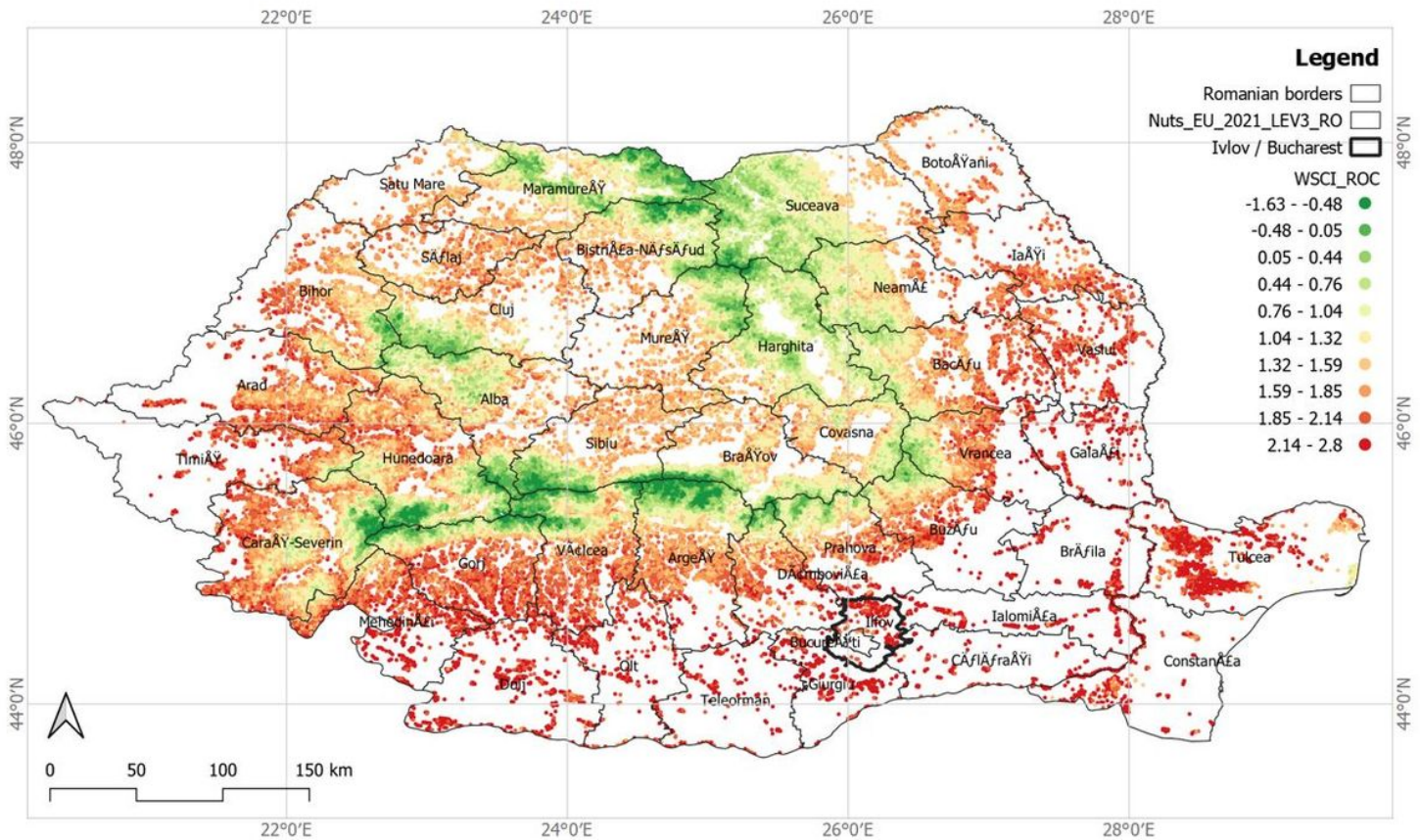


Figure 7

Wildfire spreading capacity map of vegetated surfaces on Romania (WSCI_ROC) with the highlighted metropolitan area of Ilfov. Note: The designations employed and the presentation of the material on this map do not imply the expression of any opinion whatsoever on the part of Research Square concerning the legal status of any country, territory, city or area or of its authorities, or concerning the delimitation of its frontiers or boundaries. This map has been provided by the authors.

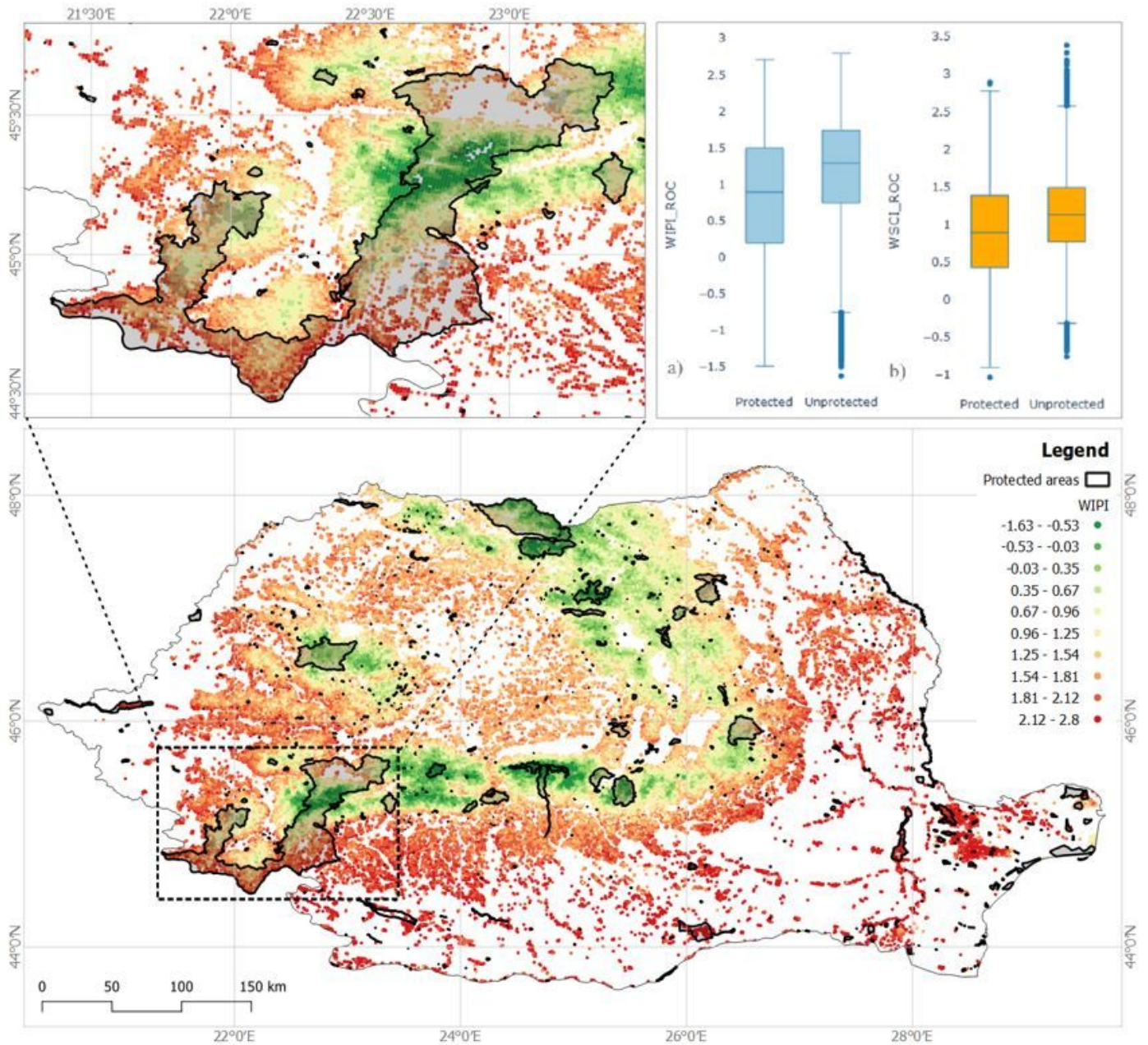


Figure 8

Wildfire spreading risk exposure map of protected areas in Romania, and comparative box plot of WIPI_ROC (a) and WSCI_ROC (b) value distribution between protected and unprotected vegetated surfaces in Romania. Note: The designations employed and the presentation of the material on this map do not imply the expression of any opinion whatsoever on the part of Research Square concerning the legal status of any country, territory, city or area or of its authorities, or concerning the delimitation of its frontiers or boundaries. This map has been provided by the authors.

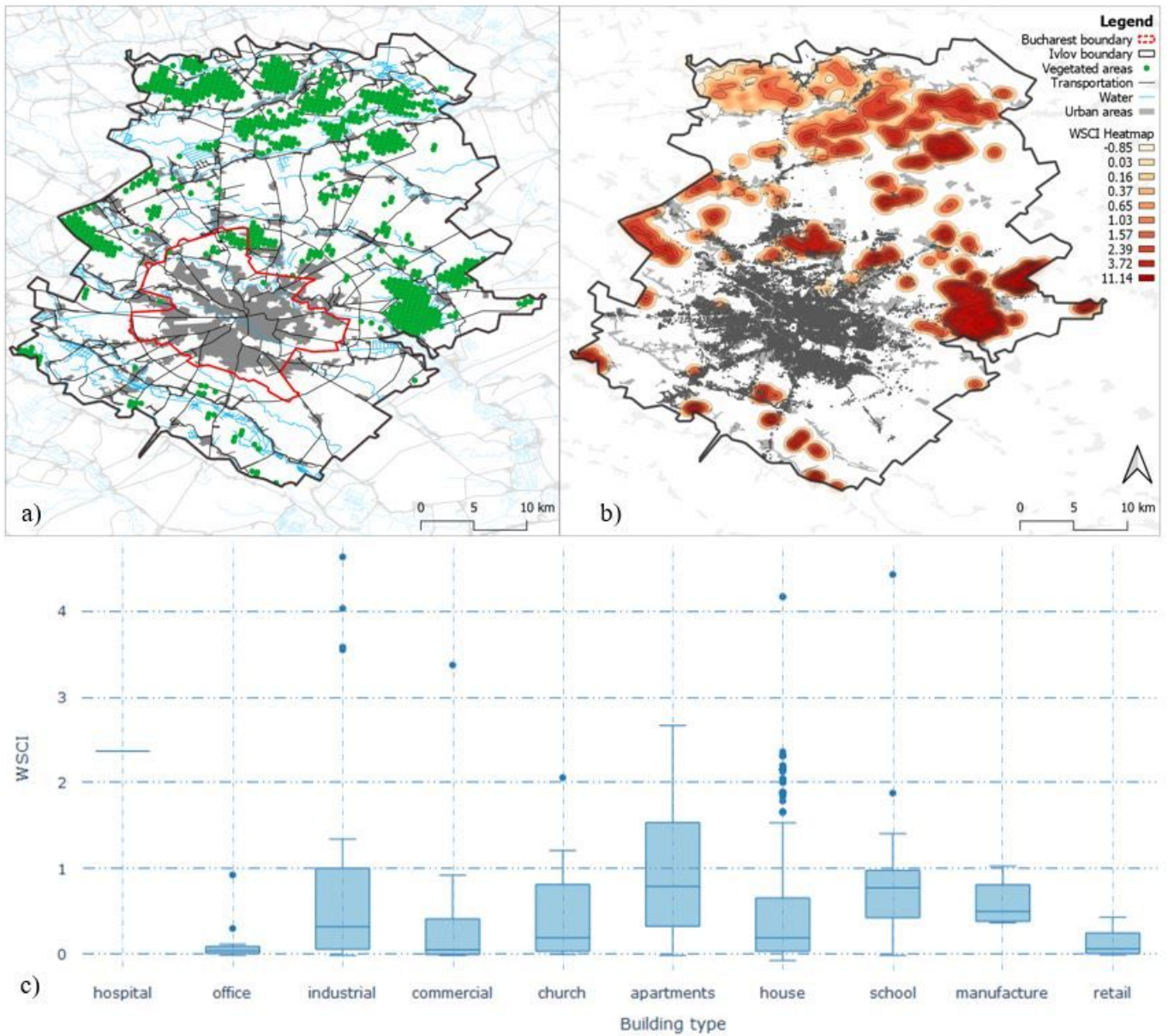


Figure 9

Wildfire exposure map of existing urban fabric (b) within Ilfov and Bucharest (a), and box plot of WSCI_cum distribution per building type of exposed structures (c). Note: The designations employed and the presentation of the material on this map do not imply the expression of any opinion whatsoever on the part of Research Square concerning the legal status of any country, territory, city or area or of its authorities, or concerning the delimitation of its frontiers or boundaries. This map has been provided by the authors.

Supplementary Files

This is a list of supplementary files associated with this preprint. Click to download.

- [NSRWildfiresinRomaniaSUPPLEMENTARY.docx](#)